Helix Waveguide Theory and Application

By HANS-GEORG UNGER

(Manuscript received March 31, 1958)

Generalized telegraphist's equations have been derived for curved helix waveguide and coefficients obtained for conversion from normal modes of the helix waveguide to normal modes of the metallic waveguide. A radial wave impedance at the helix interface is used to calculate the effect of composite jacket structures. Three different applications of the helix waveguide for circular electric wave transmission are discussed: As a mode filter, the helix waveguide should have a lossy jacket which causes a high transmission loss for all unwanted modes. For sharp intentional bends with tapered curvature, the helix waveguide should have a jacket of low-loss dielectric material surrounded by a highly conducting coaxial shield. For an all-helix waveguide, in order to reduce both mode conversion-reconversion effects at imperfections and loss in curvature the jacket should be medium lossy and also surrounded by a metallic shield. The distance between helix and shield should in all applications be about a quarter of the radial wavelength in the material. Measurements on unwanted mode transmission and TE_{01} curvature loss confirm the analysis.

I. INTRODUCTION

Helix waveguide consisting of closely wound insulated copper wire covered with a jacket of dielectric material and surrounded by a coaxial metallic shield has been shown to be useful as a communication medium.[1] The low-pitch helix gives to this structure the low-loss characteristics of solid copper-wall waveguide for circular-electric waves. All other modes of propagation, however, suffer a change of their field configuration and propagation constants, depending on the properties of the outside jacket and shield.[2]

There are two distinctive applications of the helix waveguide for circular electric wave transmission, requiring different but definite properties of jacket and shield. One is the use of helix waveguide in short sections inserted as mode filters in an otherwise conventional waveguide, to reduce the mode conversion-reconversion distortion of TE_{01} propagation. For this application the attenuation constant of all unwanted modes should be made as high as possible by choosing a material with a certain loss factor for the jacket. The other application is to transmit the circular-electric wave around sharp intentional bends.[3] In this case the jacket of the helix waveguide should be as low in loss as possible and the distance between helix and outer metallic shield should be chosen so as to minimize mode conversion and dissipation loss in bends.

Beyond this, a third and probably the most important application is the all-helix waveguide as transmission medium. In this case, high unwanted mode attenuation as well as low TE_{01} loss in bends is desired. A compromise between the helix waveguide for mode filters and the helix waveguide for sharp bends has to be met by choosing a medium lossy jacket and the proper distance between jacket and shield. This compromise will be made on the basis of tolerances. While the manufacturing tolerances call for a mode-filtering helix waveguide, the laying tolerances call for low TE_{01} loss in random curvature.

In order to design these different types of helix waveguide, we must analyze the propagation characteristics of both the circular electric mode and the unwanted modes in the general structure of helix surrounded by lossy jacket and metallic shield with both a straight and a curved axis. In the following two sections two different approaches to this problem will be presented. Both of them make use of Schelkunoff's generalized telegraphist's equations for waveguides.[4] The propagation in the curved helix waveguide is represented by a set of coupled modes of propagation. But the set of modes used in the first approach is different from the one used in the second approach. In Sections II and III the generalized telegraphist's equations are derived. In Section IV the problem of a composite jacket structure is reduced to a radial transmission line problem. The theory is applied to practical helix waveguide problems in Section V, and conclusions are actually given there. The reader interested only in design and application of helix waveguide is therefore referred immediately to Sections IV and V.

II. REPRESENTATION IN TERMS OF NORMAL MODES OF THE METALLIC WAVEGUIDE

To obtain generalized telegraphist's equations the field at any cross section of the curved helix waveguide is represented as a superposition of the fields of a certain set of normal modes. A current and a voltage amplitude are associated with each normal mode and the currents and voltages, after Maxwell's equations and the boundary conditions of the curved helix waveguide are applied, are found to satisfy an infinite set of generalized telegraphist's equations. The coupling terms in these equations depend upon the curvature of the guide axis and the jacket structure. The choice of normal modes may be arbitrary, but, in this case, it seems most appropriate to choose the normal modes of a straight circular waveguide with perfectly conducting walls. It appears that, with this choice of modes, the generalized telegraphist's equations will also solve the problem of mode conversion at an abrupt or gradual transition from metallic waveguide to helix waveguide. Also, it will be possible to analyze mode conversion at all those imperfections of the helix waveguide, for which the mode conversion in a metallic waveguide is known.

The natural coordinate system (r, φ, z) for a curved circular waveguide is toroidal (Fig. 1), where z is the distance measured along the curved axis of the guide and r and φ are polar coordinates in a plane normal to the axis of the guide, with origin at the guide axis. The lines $\varphi = 0$ and $\varphi = \pi$ lie in the plane of the bend. The inner radius of the guide is denoted by a and the radius of the bend by R.

For the moment, (r, φ, z) are regarded as general orthogonal curvilinear coordinates (u, v, w) by letting

$$u = r \qquad v = \varphi \qquad w = z. \tag{1}$$

The element of length in this system is

$$ds^2 = e_1^2 du^2 + e_2^2 dv^2 + e_3^2 dw^2, \tag{2}$$

where

$$e_1 = 1; \qquad e_2 = r; \qquad e_3 = 1 + \xi \tag{3}$$

and

$$\xi = \frac{r}{R} \cos \varphi. \tag{4}$$

For a field with time dependence $e^{j\omega t}$, Maxwell's equations are:

$$\frac{1}{e_2 e_3}\left[\frac{\partial}{\partial v}(e_3 E_w) - \frac{\partial}{\partial w}(e_2 E_v)\right] = -j\omega\mu H_u, \tag{5}$$

$$\frac{1}{e_3 e_1}\left[\frac{\partial}{\partial w}(e_1 E_u) - \frac{\partial}{\partial u}(e_3 E_w)\right] = -j\omega\mu H_v, \tag{6}$$

$$\frac{1}{e_1 e_2}\left[\frac{\partial}{\partial u}(e_2 E_v) - \frac{\partial}{\partial v}(e_1 E_u)\right] = -j\omega\mu H_w, \tag{7}$$

$$\frac{1}{e_2 e_3}\left[\frac{\partial}{\partial v}(e_3 H_w) - \frac{\partial}{\partial w}(e_2 H_v)\right] = j\omega\epsilon E_u, \tag{8}$$

$$\frac{1}{e_3 e_1}\left[\frac{\partial}{\partial w}(e_1 H_u) - \frac{\partial}{\partial u}(e_3 H_w)\right] = j\omega\epsilon E_v, \tag{9}$$

$$\frac{1}{e_1 e_2}\left[\frac{\partial}{\partial u}(e_2 H_v) - \frac{\partial}{\partial v}(e_1 H_u)\right] = j\omega\epsilon E_w. \tag{10}$$

The permeability μ and the permittivity ϵ are those of free space in the waveguide interior, but between helix and shield ϵ is determined by the choice of the jacket. If there is dissipation in the jacket it is complex.

To convert Maxwell's equations into generalized telegraphist's equations we introduce the field components of the normal modes of our choice. Each mode is described by a transverse field distribution pattern $T(u, v)$, which satisfies

$$\nabla^2 T = \frac{1}{e_1 e_2}\left[\frac{\partial}{\partial u}\left(\frac{e_2}{e_1}\frac{\partial T}{\partial u}\right) + \frac{\partial}{\partial v}\left(\frac{e_1}{e_2}\frac{\partial T}{\partial v}\right)\right] = -\chi^2 T, \tag{11}$$

where χ is a separation constant which has discrete values for the various TE and TM modes. Brackets will be used for TE modes and parentheses for TM modes. Thus, the function corresponding to the nth TE mode is denoted by $T_{[n]}(u, v)$ and the separation constant by $\chi_{[n]}$ with the subscript in brackets. The function corresponding to the nth TM mode is denoted by $T_{(n)}(u, v)$ and the separation constant by $\chi_{(n)}$, with the subscript in parenthesis. The normal derivative of $T_{[n]}$ vanishes on the boundary $u = a$, while $T_{(n)}$ itself vanishes at $u = a$.

The T functions are assumed to be so normalized that

$$\int_S (\text{grad } T)(\text{grad } T)\, dS = \int_S (\text{flux } T)(\text{flux } T)\, dS = \chi^2 \int_S T^2\, dS = 1, \tag{12}$$

where S is the cross section of the guide inside the helix.

With the definition of the gradient and flux of T:

$$\text{grad}_u\, T = \frac{\partial T}{e_1 \partial u}, \qquad \text{grad}_v\, T = \frac{\partial T}{e_2 \partial v},$$
$$\text{flux}_u\, T = \frac{\partial T}{e_2 \partial v}, \qquad \text{flux}_v\, T = -\frac{\partial T}{e_1 \partial u}, \tag{13}$$

various orthogonality relations exist among the T functions:

$$
\begin{gathered}
\int_S T_{(n)} T_{(m)}\, dS = \int_S T_{[n]} T_{[m]}\, dS = 0, \\
\int_S (\text{grad } T_{(n)})(\text{grad } T_{(m)})\, dS = \int_S (\text{flux } T_{(n)})(\text{flux } T_{(m)})\, dS = 0, \\
\int_S (\text{grad } T_{[n]})(\text{grad } T_{[m]})\, dS = \int_S (\text{flux } T_{[n]})(\text{flux } T_{[m]})\, dS = 0
\end{gathered}
\tag{14}
$$

if $m \neq n$, and

$$
\begin{aligned}
\int_S (\text{grad } T_{(n)})(\text{flux } T_{[m]})\, dS &= \int_S (\text{grad } T_{[n]})(\text{flux } T_{(m)})\, dS \\
&= \int_S (\text{grad } T_{(n)})(\text{flux } T_{(m)})\, dS = 0
\end{aligned}
\tag{15}
$$

for all m and n. We now assume series expansions of the field components in terms of the functions $T(u, v)$, with coefficients I and V depending on w:

$$
\begin{aligned}
E_u &= \sum_n \left[V_{(n)} \frac{\partial T_{(n)}}{e_1 \partial u} + V_{[n]} \frac{\partial T_{[n]}}{e_2 \partial v} \right], \\
E_v &= \sum_n \left[V_{(n)} \frac{\partial T_{(n)}}{e_2 \partial v} - V_{[n]} \frac{\partial T_{[n]}}{e_1 \partial u} \right], \\
H_u &= \sum_n \left[-I_{(n)} \frac{\partial T_{(n)}}{e_2 \partial v} + I_{[n]} \frac{\partial T_{[n]}}{e_1 \partial u} \right], \\
H_v &= \sum_n \left[I_{(n)} \frac{\partial T_{(n)}}{e_1 \partial u} + I_{[n]} \frac{\partial T_{[n]}}{e_2 \partial v} \right].
\end{aligned}
\tag{16}
$$

With the T functions, the field components in (16) are only defined inside of the helix for $u < a$. The effects of jacket and shield (at radius b) are taken into account by the boundary conditions:

$$
E_v = 0, \tag{17}
$$

$$
E_w = -ZH_v \tag{18}
$$

at the helix. In these conditions, the low-pitch helix has been replaced by an anisotropically conducting sheath, and jacket and shield by a wall impedance Z. Later on in this paper we shall discuss how to calculate this wall impedance and even how to take the effect of finite wire size of the helix into account by modifying Z.

The boundary condition (17) is satisfied by the individual terms of the series for E_v .

To transform Maxwell's equations into generalized telegraphist's equations the series expansions (16) are substituted for the field components in (5) through (10). Then certain combinations of these equations are integrated over the cross section and advantage is taken of the orthogonality relation (14) and (15). For example, substituting from (16) into (5) and (6), adding

$$-\frac{e_3}{e_2}\frac{\partial T_{(m)}}{\partial v} \text{ times (5)} \qquad \text{and} \qquad \frac{e_3}{e_1}\frac{\partial T_{(m)}}{\partial u} \text{ times (6)}$$

and integrating over the cross section, we obtain:

$$\frac{dV_{(m)}}{dw} + j\omega\mu \sum_n \left[I_{(n)} \int_S e_3(\text{grad } T_{(n)})(\text{grad } T_{(m)})\, dS \right.$$
$$\left. + I_{[n]} \int_S e_3(\text{flux } T_{[n]})(\text{grad } T_{(m)})\, dS \right] \tag{19}$$
$$= \int_S (\text{grad } e_3E_w)(\text{grad } T_{(m)})\, dS.$$

The right-hand side can be integrated by parts according to Green's theorem:

$$a \int_0^{2\pi} e_3E_w \frac{\partial T_{(m)}}{\partial u}\bigg|_a dv - \int_S e_3E_w \text{ div grad } T_{(m)}\, dS.$$

In the first term of this expression, E_w is replaced by H_v through the boundary condition (18) and, for H_v in turn, the series expansion of (16) is substituted:

$$a \int_0^{2\pi} e_3E_w \frac{\partial T_{(m)}}{\partial u}\bigg|_a dv = -aZ \sum_n \left[I_{(n)} \int_0^{2\pi} \frac{e_3}{e_1}\frac{\partial T_{(n)}}{\partial u}\frac{\partial T_{(m)}}{\partial u}\, dv \right.$$
$$\left. + I_{[n]} \int_0^{2\pi} \frac{e_3}{e_2}\frac{\partial T_{[n]}}{\partial v}\frac{\partial T_{(m)}}{\partial u}\, dv \right].$$

In the second term of the foregoing expression, E_w is replaced by H_v and H_u through (10) and, for H_v and H_u in turn, the series expansion of (16) is substituted:

$$j\omega\epsilon E_w = -\sum_n I_{(n)}\chi_{(n)}{}^2 T_{(n)}. \tag{20}$$

Therefore:

$$-\int_S e_3E_w \text{ div grad } T_{(m)}\, dS = \frac{j}{\omega\epsilon} \sum_n I_{(n)}\chi_{(n)}{}^2\chi_{(m)}{}^2 \int_S e_3T_{(n)}T_{(m)}\, dS.$$

where ϵ is the permittivity of the space in between wires. The corrected wall impedance is then obtained from

$$\frac{1}{Z'} = \frac{1}{Z} + j\omega\epsilon d\left(\frac{d}{D-d} - \frac{\ln 4}{\pi}\right). \tag{84}$$

Again, this expression must be substituted for the wall impedance in the characteristic equation (74).

All expressions for the wall impedance [(73), (76), (77), (78), (80), (84)] contain implicitly the axial propagation constant jh_n of the particular mode under consideration, and it is only through the characteristic equation (74) that this propagation constant will be determined.

In Section II, on the other hand, where the helix waveguide propagation is expressed in terms of normal modes of the solid wall guide, the wall impedance as introduced in the boundary condition (18) is not associated with a particular mode. The propagation constant jh_n remains undetermined. The boundary condition (18) cannot exactly replace a complex jacket structure.

For all cases, however, in which the modes under consideration are far from cutoff, the propagation constants are nearly equal to that of free space. We may then replace h_n by $\omega\sqrt{\mu_0\epsilon_0}$ in all expressions for the wall impedance and use them in (18) and the corresponding equations.

V. APPLICATIONS

Three different applications of the helix waveguide for circular electric wave transmission have been mentioned in the introduction. The formulae of the preceding sections will now be used to calculate the transmission properties of helix waveguide in the different applications. The theoretical values will be compared with results of measurements.

5.1 *Helix Waveguide Mode Filter*

It has been shown both theoretically and experimentally that the transmission characteristic of the circular waveguide can be substantially improved by the insertion of mode filters at intervals along the waveguide.[9] Conversion of energy to unwanted modes and reconversion at any imperfections of the waveguide seriously disturb the TE_{01} transmission characteristic. Mode filters, which provide low loss for the TE_{01} mode and high loss for all unwanted modes, greatly reduce the effects of mode conversion-reconversion by dissipating most of the converted power in unwanted modes before reconversion.

Helix waveguide has the desired properties of low TE_{0n} attenuation and high loss for all other modes. It therefore is well suited for a mode

Similarly, by adding

$$-\frac{e_3}{e_1}\frac{\partial T_{(m)}}{\partial u} \text{ times (8)} \qquad \text{and} \qquad -\frac{e_3}{e_2}\frac{\partial T_{(m)}}{\partial v} \text{ times (9)},$$

substituting from (7) for H_w and integrating over the cross section we get:

$$\frac{dI_{(m)}}{dw} = -j\omega\epsilon \sum_n \left[V_{(n)} \int_S e_3 \,(\text{grad } T_{(n)})(\text{grad } T_{(m)})\, dS + V_{[n]} \int_S e_3 \,(\text{grad } T_{(m)})(\text{flux } T_{[n]})\, dS \right]. \tag{24}$$

Finally, by adding

$$-\frac{e_3}{e_2}\frac{\partial T_{[m]}}{\partial v} \text{ times (8)} \qquad \text{and} \qquad \frac{e_3}{e_1}\frac{\partial T_{[m]}}{\partial u} \text{ times (9)},$$

again substituting from (7) for H_w and integrating over the cross section we get:

$$\begin{aligned} \frac{dI_{[m]}}{dw} = &-j\omega\epsilon \sum_n V_{[n]} \left[\int_S e_3 \,(\text{grad } T_{[n]})(\text{grad } T_{[m]}) dS - \frac{\chi_{[n]}^2 \chi_{[m]}^2}{\omega^2 \mu\epsilon} \int_S e_3 T_{[n]} T_{[m]}\, dS \right] \\ &- j\omega\epsilon \sum_n V_{(n)} \int_S e_3 \,(\text{grad } T_{(n)})(\text{flux } T_{[m]})\, dS. \end{aligned} \tag{25}$$

Equations (21), (23), (24) and (25) are generalized telegraphist's equations for the curved helix waveguide. They can be written in the following form:

$$\begin{aligned} \frac{dV_{(m)}}{dw} &= -\sum_n [Z_{(m)(n)} I_{(n)} + Z_{(m)[n]} I_{[n]}], \\ \frac{dV_{[m]}}{dw} &= -\sum_n [Z_{[m](n)} I_{(n)} + Z_{[m][n]} I_{[n]}], \\ \frac{dI_{(m)}}{dw} &= -\sum_n [Y_{(m)(n)} V_{(n)} + Y_{(m)[n]} V_{[n]}], \\ \frac{dI_{[m]}}{dw} &= -\sum_n [Y_{[m](n)} V_{(n)} + Y_{[m][n]} V_{[n]}]. \end{aligned} \tag{26}$$

The impedance and admittance coefficients are defined by

$$
\begin{aligned}
Z_{(m)(n)} &= j\omega\mu\left[\int_S e_3\,(\text{grad } T_{(n)})(\text{grad } T_{(m)})\,dS\right.\\
&\qquad \left. - \frac{\chi_{(n)}{}^2\chi_{(m)}{}^2}{\omega^2\mu\epsilon}\int_S e_3 T_{(n)} T_{(m)}\,dS + \frac{aZ}{j\omega\mu}\int_0^{2\pi}\frac{e_3}{e_1}\frac{\partial T_{(n)}}{\partial u}\frac{\partial T_{(m)}}{\partial u}\,dv\right],\\
Z_{(m)[n]} &= j\omega\mu\left[\int_S e_3\,(\text{grad } T_{(m)})(\text{flux } T_{[n]})\,dS\right.\\
&\qquad \left. + \frac{aZ}{j\omega\mu}\int_0^{2\pi}\frac{e_3}{e_2}\frac{\partial T_{[n]}}{\partial v}\frac{\partial T_{(m)}}{\partial u}\,dv\right],\\
Z_{[m](n)} &= j\omega\mu\left[\int_S e_3\,(\text{grad } T_{(n)})(\text{flux } T_{[m]})\,dS\right.\\
&\qquad \left. + \frac{Z}{j\omega\mu}\int_0^{2\pi}\frac{e_3}{e_1}\frac{\partial T_{(n)}}{\partial u}\frac{\partial T_{[m]}}{\partial v}\,dv\right],\\
Z_{[m][n]} &= j\omega\mu\left[\int_S e_3\,(\text{grad } T_{[n]})(\text{grad } T_{[m]})\,dS\right. \qquad (27)\\
&\qquad \left. + \frac{Z}{j\omega\mu}\int_0^{2\pi}\frac{e_3}{e_2}\frac{\partial T_{[n]}}{\partial v}\frac{\partial T_{[m]}}{\partial v}\,dv\right],\\
Y_{(m)(n)} &= j\omega\epsilon\int_S e_3\,(\text{grad } T_{(n)})(\text{grad } T_{(m)})\,dS,\\
Y_{(m)[n]} &= j\omega\epsilon\int_S e_3\,(\text{grad } T_{(m)})(\text{flux } T_{[n]})\,dS,\\
Y_{[m](n)} &= j\omega\epsilon\int_S e_3\,(\text{grad } T_{(n)})(\text{flux } T_{[m]})\,dS,\\
Y_{[m][n]} &= j\omega\epsilon\left[\int_S e_3\,(\text{grad } T_{[n]})(\text{grad } T_{[m]})\,dS\right.\\
&\qquad \left. - \frac{\chi_{[n]}{}^2\chi_{[m]}{}^2}{\omega^2\mu\epsilon}\int_S e_3 T_{[n]} T_{[m]}\,dS\right].
\end{aligned}
$$

We note the following symmetry properties of these coefficients:

$$
\begin{aligned}
Z_{(m)(n)} &= Z_{(n)(m)}\,, \qquad & Y_{(m)(n)} &= Y_{(n)(m)}\,;\\
Z_{[m][n]} &= Z_{[n][m]}\,, \qquad & Y_{[m][n]} &= Y_{[n][m]}\,; \qquad (28)\\
Z_{[m](n)} &= Z_{(n)[m]}\,, \qquad & Y_{[m](n)} &= Y_{(n)[m]}\,.
\end{aligned}
$$

The generalized telegraphist's equations represent an infinite set of mutually coupled transmission lines. For our purposes, it is more convenient to write the transmission-line equations not in terms of currents and voltages but in terms of the amplitudes of forward and backward travelling waves. Thus, let a and b be the amplitudes of the forward and backward waves of a typical mode at a certain cross section. The mode current and voltages are related to the wave amplitudes a and b by

$$\begin{aligned} V &= \sqrt{K}\,(a + b), \\ I &= \frac{1}{\sqrt{K}}\,(a - b), \end{aligned} \tag{29}$$

where K is the wave impedance

$$K_{(n)} = \frac{\beta_{(n)}}{\omega\epsilon}, \qquad K_{[n]} = \frac{\omega\mu}{\beta_{[n]}},$$

$$\beta_{(n)} = (\beta^2 - \chi_{(n)}^{\;2})^{1/2}, \qquad \beta_{[n]} = (\beta^2 - \chi_{[n]}^{\;2})^{1/2}, \qquad \beta^2 = \omega^2\mu\epsilon.$$

The currents and voltages in the generalized telegraphist's equations (26) are represented in terms of the travelling-wave amplitudes. The following equations for coupled travelling waves are obtained after some obvious additions and subtractions:

$$\begin{aligned} \frac{da_{(m)}}{dz} &= -\sum_n [\kappa_{(m)(n)}{}^{+}a_{(n)} + \kappa_{(m)(n)}{}^{-}b_{(n)} + \kappa_{(m)[n]}{}^{+}a_{[n]} + \kappa_{(m)[n]}{}^{-}b_{[n]}], \\ \frac{db_{(m)}}{dz} &= +\sum_n [\kappa_{(m)(n)}{}^{-}a_{(n)} + \kappa_{(m)(n)}{}^{+}b_{(n)} + \kappa_{(m)[n]}{}^{-}a_{[n]} + \kappa_{(m)[n]}{}^{+}b_{[n]}], \\ \frac{da_{[m]}}{dz} &= -\sum_n [\kappa_{[m](n)}{}^{+}a_{(n)} + \kappa_{[m](n)}{}^{-}b_{(n)} + \kappa_{[m][n]}{}^{+}a_{[n]} + \kappa_{[m][n]}{}^{-}b_{[n]}], \\ \frac{db_{[m]}}{dz} &= +\sum_n [\kappa_{[m](n)}{}^{-}a_{(n)} + \kappa_{[m](n)}{}^{+}b_{(n)} + \kappa_{[m][n]}{}^{-}a_{[n]} + \kappa_{[m][n]}{}^{+}b_{[n]}]. \end{aligned} \tag{30}$$

The κ's are coupling coefficients defined by

$$\begin{aligned} \kappa_{(m)(n)}{}^{\pm} &= \frac{1}{2}\left[\sqrt{K_{(m)}K_{(n)}}\;Y_{(m)(n)} \pm \frac{1}{\sqrt{K_{(m)}K_{(n)}}}\,Z_{(m)(n)}\right], \\ \kappa_{(m)[n]}{}^{\pm} &= \frac{1}{2}\left[\sqrt{K_{(m)}K_{[n]}}\;Y_{(m)[n]} \pm \frac{1}{\sqrt{K_{(m)}K_{[n]}}}\,Z_{(m)[n]}\right], \\ \kappa_{[m](n)}{}^{\pm} &= \frac{1}{2}\left[\sqrt{K_{[m]}K_{(n)}}\;Y_{[m](n)} \pm \frac{1}{\sqrt{K_{[m]}K_{(n)}}}\,Z_{[m](n)}\right], \\ \kappa_{[m][n]}{}^{\pm} &= \frac{1}{2}\left[\sqrt{K_{[m]}K_{[n]}}\;Y_{[m][n]} \pm \frac{1}{\sqrt{K_{[m]}K_{[n]}}}\,Z_{[m][n]}\right]. \end{aligned} \tag{31}$$

In these definitions the plus signs are taken together, as are the minus signs.

To examine the coupling coefficients, we introduce field functions of the normal modes of the circular guide with perfectly conducting walls. We shall use the customary double-subscript notation, but shall continue to denote TM waves with parentheses and TE waves with brackets:

$$
\begin{aligned}
T_{(nm)} &= \sqrt{\frac{\epsilon_n}{\pi}}\, \frac{J_n(\chi_{(nm)}r)\sin n\varphi}{k_{(nm)}J_{n-1}(k_{nm})}, \\
T_{[nm]} &= \sqrt{\frac{\epsilon_n}{\pi}}\, \frac{J_n(\chi_{[nm]}r)\cos n\varphi}{(k_{[nm]}{}^2 - n^2)^{1/2}J_n(k_{nm})},
\end{aligned} \tag{32}
$$

where

$$
\begin{aligned}
k_{(nm)} &= \chi_{(nm)}a, \qquad J_n(k_{(nm)}) = 0; \\
k_{[nm]} &= \chi_{[nm]}a, \qquad J_n'(k_{[nm]}) = 0
\end{aligned} \tag{33}
$$

and

$$
\begin{aligned}
\epsilon_n &= 1, \qquad n = 0, \\
\epsilon_n &= 2, \qquad n \neq 0.
\end{aligned} \tag{34}
$$

Introducing (32) into (27) and these in turn into (31), the coupling coefficients are calculated.

There are two different causes of coupling between the metallic guide normal modes. One is the finite wall impedance Z of the helix waveguide; we shall continue to denote the corresponding coupling coefficient with κ. The other is the curvature of the guide axis; we shall denote the corresponding coupling coefficient with jc. The coefficients of curvature coupling jc turn out to be purely imaginary.

The κ's in (31) which have equal subscripts may be regarded as propagation constants of typical TM or TE modes which have been modified by the finite wall impedance Z. It turns out that these modified propagation constants do not depend on the curvature:

$$
\begin{aligned}
\kappa_{(nm)(nm)} &= \gamma_{(nm)} = j\beta_{(nm)} + \frac{\epsilon_n}{2a}\frac{Z}{K_{(nm)}}, \\
\kappa_{[nm][nm]} &= \gamma_{[nm]} = j\beta_{[nm]} + \frac{\epsilon_n}{2a}\frac{n^2}{k_{[nm]}{}^2 - n^2}\frac{Z}{K_{[nm]}}.
\end{aligned} \tag{35}
$$

For all other κ's we find that the wall impedance causes coupling only between modes of equal subscript n in (32). The corresponding coupling coefficients are:

$$\kappa_{(nm)(np)}{}^{+} = \frac{\epsilon_n}{2a} \frac{Z}{\sqrt{K_{(nm)}K_{(np)}}},$$

$$\kappa_{(nm)[np]}{}^{+} = \kappa_{[np](nm)}{}^{+} = -\frac{\epsilon_n}{2a} \frac{n}{\sqrt{k_{[np]}{}^2 - n^2}} \frac{Z}{\sqrt{K_{(nm)}K_{[np]}}}, \quad (36)$$

$$\kappa_{[nm][np]}{}^{+} = \frac{\epsilon_n}{2a} \frac{n^2}{\sqrt{k_{[nm]}{}^2 - n^2}\sqrt{k_{[np]}{}^2 - n^2}} \frac{Z}{\sqrt{K_{[nm]}K_{[np]}}}.$$

The curvature of the guide axis causes coupling only between modes which have a subscript n in (32) differing by one. The corresponding coupling coefficients are the same as in the curved circular guide with perfectly conducting walls.[5] We obtain, for example,

$$c_{[01](11)}{}^{+} = \frac{\beta}{\sqrt{2}\, k_{[01]}} \frac{a}{R},$$

$$c_{[01](1m)}{}^{+} = 0 \qquad \text{for } m \neq 1,$$

$$c_{[01][1m]}{}^{+} = \frac{\sqrt{2}\, k_{[01]}k_{[1m]}{}^2}{\sqrt{k^2_{[1m]} - 1}(k^2_{[01]} - k^2_{[1m]})^2}\left(\frac{\sqrt{2}\,\beta^2a^2 - k^2_{[01]} - k^2_{[1m]}}{a^2\sqrt{2\beta_{[01]}\beta_{[1m]}}} + \sqrt{\beta_{[01]}\beta_{[1m]}}\right)\frac{a}{R}. \quad (37)$$

The curvature coupling between TE_{01} and all other modes does not depend on the finite wall impedance of the helix waveguide.

There is some combined curvature and wall-impedance coupling between certain higher order modes. However, for TE_{01} transmission in the helix waveguide, this is of no interest.

To apply the preceding analysis to practical problems we need consider only the forward waves, since the relative power coupled from the forward waves into the backward waves is quite small. After the b's and κ^{-}'s have been omitted, (30) can conveniently be written in matrix form:

$$A' = -MA. \quad (38)$$

If we designate the amplitude of the TE_{01} by a_0 and let the remaining a's represent the amplitudes of the modes which are coupled to TE_{01} in the curved helix waveguide in order of their cut-off frequencies, then, in a somewhat simplified notation, the matrices in (38) are defined by:

$$A' = \frac{dA}{dz}, \qquad A = \begin{bmatrix} a_0 \\ a_1 \\ a_2 \\ \cdot \\ \cdot \\ \cdot \end{bmatrix}, \qquad M = \begin{bmatrix} j\beta_0 & jc_{01} & jc_{02} & \cdots \\ jc_{01} & \kappa_{11} & \kappa_{12} & \cdots \\ jc_{02} & \kappa_{12} & \kappa_{22} & \cdots \\ \cdot & \cdot & \cdot & \\ \cdot & \cdot & \cdot & \\ \cdot & \cdot & \cdot & \end{bmatrix}. \tag{39}$$

If both the c's and off-diagonal κ's were small, the solution of (38) could be written down as a perturbation of the propagation in the straight metallic waveguide. This is usually not the case. In gentle bends such as we are interested in here, however, the curvature coupling is orders of magnitude smaller than the wall impedance coupling between the modes. Therefore, it is convenient to split M into $M_h + M_c$, where M_h is the straight helix waveguide matrix and M_c takes the curvature effects into account:

$$M_h = \begin{bmatrix} j\beta_0 & 0 & 0 & \cdots \\ 0 & \kappa_{11} & \kappa_{12} & \cdots \\ 0 & \kappa_{12} & \kappa_{22} & \cdots \\ \cdot & \cdot & \cdot & \\ \cdot & \cdot & \cdot & \\ \cdot & \cdot & \cdot & \end{bmatrix}, \qquad M_c = \begin{bmatrix} 0 & jc_{01} & jc_{02} & \cdots \\ jc_{01} & 0 & 0 & \cdots \\ jc_{02} & 0 & 0 & \cdots \\ \cdot & \cdot & \cdot & \\ \cdot & \cdot & \cdot & \\ \cdot & \cdot & \cdot & \end{bmatrix}. \tag{40}$$

The effect of curvature can be calculated by a perturbation method, but

$$A' = M_h A \tag{41}$$

will have to be solved more rigorously. To do this, we diagonalize M_h by the transformation

$$A = LW, \tag{42}$$

where L is the modal matrix[6] of M_h. Since M_h is symmetrical, we have $L_t = L^{-1}$ and the transformation of M_h to the diagonal form of its latent roots[6] reads:

$$L_t M_h L = \Gamma.$$

In

$$\Gamma = \begin{bmatrix} \gamma_0 & 0 & 0 & \cdots \\ 0 & \gamma_1 & 0 & \cdots \\ 0 & 0 & \gamma_2 & \cdots \\ \cdot & \cdot & \cdot & \\ \cdot & \cdot & \cdot & \\ \cdot & \cdot & \cdot & \end{bmatrix} \tag{43}$$

the γ's are solutions of the characteristic equation

$$\begin{vmatrix} j\beta_0 - \gamma & 0 & 0 & \cdots \\ 0 & \kappa_{11} - \gamma & \kappa_{12} & \cdots \\ 0 & \kappa_{12} & \kappa_{22} - \gamma & \cdots \\ \cdot & \cdot & \cdot & \\ \cdot & \cdot & \cdot & \\ \cdot & \cdot & \cdot & \end{vmatrix} = 0. \tag{44}$$

A typical element of the modal matrix L of M_h is defined by:

$$l_{ks} = \frac{\overset{s}{q}_{ik}}{\sqrt{\left(\overset{s}{q}_{i1}\right)^2 + \left(\overset{s}{q}_{i2}\right)^2 + \cdots \left(\overset{s}{q}_{in}\right)^2}}, \tag{45}$$

where $\overset{s}{q}_{ik}$ is the cofactor of an element of the determinant in (44) for the root $\gamma = \gamma_s$. The index i is arbitrary as long as it is different from zero but it must, of course, be the same for the determination of all the l's for a given s.

Physically, (42) means transformation to the normal modes of the straight helix waveguide, and the γ's are the propagation constants of the normal modes in the straight helix waveguide. The elements of L in (42) describe the conversion of normal modes of the straight helix waveguide into normal modes of the metallic waveguide. The TE_{01} amplitude and propagation constants are, of course, not changed by this transformation:

$$w_0 = a_0, \qquad \gamma_0 = j\beta_0 .$$

Introducing the normal modes w into (38), we get for the propagation in the curved helix waveguide

$$W' = -(\Gamma + C)W, \tag{46}$$

where $C = L_t M_c L$ represents the effect of curvature in the helix waveguide. The elements of C are the coefficients of coupling between the normal modes of the straight helix waveguide in curved sections, and C is a symmetrical matrix with nonvanishing elements only in the first row and first column. A typical element is given by

$$c_s = j(c_{01}l_{1s} + c_{02}l_{2s} + c_{03}l_{32} + \cdots). \tag{47}$$

Since Γ in (46) is diagonal, and since the elements of C are small enough to justify a perturbation calculation, the problem of the curved helix waveguide is formally solved.

The perturbation calculation for the curved guide assumes, as usual, that the coupling from TE_{01} to all other modes w is small. Then it is sufficient to consider only coupling between TE_{01} and one of the other modes at a time and to add up all these coupling effects. The TE_{01} propagation in a helix waveguide, even of nonuniform curvature, may be calculated this way.[3]

For a helix waveguide of uniform curvature our matrix notation may be used. As before with the straight helix waveguide, we now transform to the normal modes of the curved helix waveguide. The propagation constants of these curved-guide normal modes are the solution of the characteristic equation:

$$\begin{vmatrix} \gamma - \gamma_0 & c_1 & c_2 & \cdots \\ c_1 & \gamma - \gamma_1 & 0 & \cdots \\ c_2 & 0 & \gamma - \gamma_2 & \cdots \\ \vdots & \vdots & \vdots & \end{vmatrix} = 0. \tag{48}$$

Approximate solutions of this equation for

$$\left| \frac{c_s}{\gamma_n - \gamma_s} \right| \ll 1$$

are perturbations of the propagation constants γ_s of normal modes of the straight helix waveguide. In particular, we get for the perturbed propagation constant of the TE_{01} mode:

$$\gamma = \gamma_0 + \sum_s \frac{c_s^2}{\gamma_0 - \gamma_s}. \tag{49}$$

The modal matrix of $(\Gamma + C)$ transforms from the normal modes of the curved guide to those of the straight guide. Its elements give the mode conversion at the junction from curved to straight guide. A typical element of this modal matrix is given by an expression like (45) or to a sufficient approximation:

$$l_{0s} = \frac{c_s}{\gamma_0 - \gamma_s}. \tag{50}$$

The propagation constants γ_s in (49) and (50) are those of the normal modes in the helix waveguide. To obtain them, the characteristic equation (44), a polynomial of infinite degree in γ, has to be solved.

For a low wall-impedance jacket, approximate solutions of (44) may be used which, like (49), are perturbations of the metallic waveguide propagation constants. In general, (44) may be reduced to a polynomial of finite degree by omitting modes of higher order which have little effect on the lower order modes. Even so, we are usually left with the formidable problem of solving a polynomial of high degree.

To avoid the problem associated with the transformation from metallic guide normal modes to helix guide normal modes we must start with the helix waveguide normal modes and write the generalized telegraphist's equations in terms of normal modes of the helix waveguide.

III. REPRESENTATION IN TERMS OF NORMAL MODES OF THE HELIX WAVEGUIDE

Normal modes of the straight helix waveguide have been analyzed elsewhere.[2] To adapt this analysis to our representation we shall repeat and generalize the boundary value problem here. The waveguide structure we consider is shown in Fig. 1. The anisotropic conducting sheath,

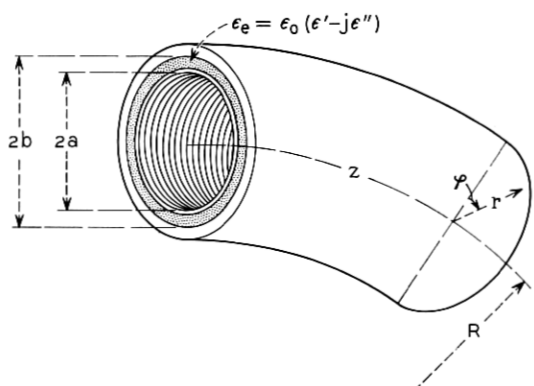

Fig. 1 — Coordinates used in bend in shielded helix waveguide.

which represents the closely wound helix, is surrounded by a dielectric jacket and a coaxial metallic shield.

The electromagnetic field in the helix waveguide can be derived from two sets of scalar functions T_n and T_n' given by

$$\begin{aligned} T_n &= N_n J_p(\chi_n r) \sin p\varphi \\ T_n' &= N_n J_p(\chi_n r) \cos p\varphi \end{aligned} \quad \text{for } 0 < r < a, \tag{51a}$$

and

$$T_n = N_n \frac{\chi_n^2}{\chi_n^{e^2}} J_p(k_n) \frac{H_p^{(2)}(\chi_n^e r) - cH_p^{(1)}(\chi_n^e r)}{H_p^{(2)}(k_n^e) - cH_p^{(1)}(k_n^e)} \sin p\varphi$$

$$\text{for } a < r < b. \tag{51b}$$

$$T_n' = N_n \frac{\chi_n^2}{\chi_n^{e^2}} J_p(k_n) \frac{H_p^{(2)}(\chi_n^e r) - c'H_p^{(1)}(\chi_n^e r)}{H_p^{(2)}(k_n^e) - c'H_p^{(1)}(k_n^e)} \cos p\varphi$$

Being solutions of the wave equation, the T functions satisfy (11). The field components are written in terms of these field functions, using the coordinates (u, v, w) of (1):

$$\begin{aligned} E_u &= \sum_n V_n \left[\frac{\partial T_n}{e_1 \partial u} + d_n \frac{\partial T_n'}{e_2 \partial v}\right], \\ E_v &= \sum_n V_n \left[\frac{\partial T_n}{e_2 \partial v} - d_n \frac{\partial T_n'}{e_1 \partial u}\right], \\ H_u &= \sum_n - I_n \left[\frac{\partial T_n}{e_2 \partial v} - d_n \frac{h_n^2}{k^2} \frac{\partial T_n'}{e_1 \partial u}\right] \frac{\epsilon}{\epsilon_0}, \\ H_v &= \sum_n I_n \left[\frac{\partial T_n}{e_1 \partial u} + d_n \frac{h_n^2}{k^2} \frac{\partial T_n'}{e_2 \partial v}\right] \frac{\epsilon}{\epsilon_0}. \end{aligned} \tag{52}$$

Substituting from (52) into (7) and (10) and taking advantage of (11), we get for the longitudinal field components:

$$\begin{aligned} H_w &= j\omega\epsilon \sum_n V_n \, d_n \frac{\chi_n^2}{k^2} T_n', \\ E_w &= j\omega\mu \sum_n I_n \frac{\epsilon}{\epsilon_0} \frac{\chi_n^2}{k^2} T_n , \end{aligned} \tag{53}$$

where ϵ and $k = \omega\sqrt{\mu\epsilon}$ are permittivity and intrinsic propagation constant of the medium in a particular cross-sectional part of the guide. They have constant but different values for the different cross-sectional parts of the guide, and ϵ_0 is the permittivity of the empty helix interior.

The quantities d_n, c and c' and the separation constants χ_n and χ_n^e are chosen so that the boundary conditions of the shielded helix waveguide

$$\begin{aligned} E_v &= 0 && \text{at helix and shield,} \\ E_w &= 0 && \text{at shield,} \\ E_{w\text{interior}} &= E_{w\text{exterior}} && \text{at helix,} \\ H_{v\text{interior}} &= H_{v\text{exterior}} && \text{at helix} \end{aligned} \tag{54}$$

are satisfied by the individual terms of (52). Only then do the individual terms of (52) represent normal modes of the shielded helix waveguide. From $E_v = 0$ at the helix:

$$d_n = \left.\frac{\dfrac{\partial T_n}{e_2 \partial v}}{\dfrac{\partial T_n'}{e_1 \partial u}}\right|_{u=a}. \tag{55}$$

From $E_w = 0$ at the shield:

$$c = \frac{H_p^{(2)}(\rho k_n^e)}{H_p^{(1)}(\rho k_n^e)}. \tag{56}$$

From $E_v = 0$ at the shield:

$$c' = \frac{H_p^{(2)\prime}(\rho k_n^e)}{H_p^{(1)\prime}(\rho k_n^e)}, \tag{57}$$

where $\rho = b/a$, $k_n^e = \chi_n^e a$, and $k_n = \chi_n a$. The prime at the Bessel functions denotes differentiation with respect to the argument. The condition of E_w being continuous across the helix boundary is satisfied by virtue of the formulation of the T functions in (51). The remaining condition of H_v being continuous across the boundary leads to the following (characteristic) equation of the shielded helix waveguide:

$$\begin{aligned} \frac{J_p'(k_n)}{J_p(k_n)} - \frac{p^2}{k_n^2}\frac{h_n^2}{k^2}\frac{J_p(k_n)}{J_p'(k_n)} = \frac{\epsilon_e}{\epsilon_0}\frac{k_n}{k_n^e}\Bigg[& \frac{H_p^{(2)\prime}(k_n^e) - cH_p^{(1)\prime}(k_n^e)}{H_p^{(2)}(k_n^e) - cH_p^{(1)}(k_n^e)} \\ & - \frac{p^2}{k_n^{e2}}\frac{h_n^2}{k_e^2}\frac{H_p^{(2)}(k_n^e) - c'H_p^{(1)}(k_n^e)}{H_p^{(2)\prime}(k_n^e) - c'H_p^{(1)\prime}(k_n^e)}\Bigg]. \end{aligned} \tag{58}$$

The characteristic equation, together with

$$\begin{aligned} k_n^2 &= (k^2 - h_n^2)a^2, \\ k_n^{e2} &= (k_e^2 - h_n^2)a^2 \end{aligned} \tag{59}$$

determines the separation constants k_n and k_n^e. The transverse field components of any two different modes are orthogonal to each other in that

$$\frac{1}{V_n I_m}\int_S (E_{tn} \times H_{tm})\, dS$$
$$= \int_S \frac{\epsilon}{\epsilon_0}\left[\left(\frac{\partial T_n}{e_1\partial u} + d_n \frac{\partial T_n'}{e_2\partial v}\right)\left(\frac{\partial T_m}{e_1\partial u} + d_m \frac{h_m^2}{k^2}\frac{\partial T_m'}{e_2\partial v}\right)\right. \qquad (60)$$
$$\left. + \left(\frac{\partial T_n}{e_2\partial v} - d_n \frac{\partial T_n'}{e_1\partial u}\right)\left(\frac{\partial T_m}{e_2\partial v} - d_m \frac{h_m^2}{k^2}\frac{\partial T_m'}{e_1\partial u}\right)\right] dS$$
$$= \delta_{nm}\,.$$

The integration is to be extended over the entire cross section. The quantity δ_{nm} is the Kronecker delta. To satisfy (60) for $n = m$ requires the normalization N_n to have a certain value. Both (60) and N_n are calculated in the Appendix.

We have now determined all quantities in (51) and (52) except the current and voltage coefficients. To find relations for them we substitute (52) for the field components into Maxwell's equations and convert to generalized telegraphist's equations. We add

$$-e_3\left(\frac{\partial T_m}{e_2\partial v} - d_m \frac{h_m^2}{k^2}\frac{\partial T_m'}{e_1\partial u}\right)\frac{\epsilon}{\epsilon_0} \text{ times } (5)$$

and

$$e_3\left(\frac{\partial T_m}{e_1\partial u} + d_m \frac{h_m^2}{k^2}\frac{\partial T_m'}{e_2\partial v}\right)\frac{\epsilon}{\epsilon_0} \text{ times } (6)$$

and integrate over the cross section. Using (11) and (60) and the boundary conditions of (54), the result is:

$$\frac{dV_m}{dw} + j\frac{h_m^2}{\omega\epsilon_0} I_m = -j\omega\mu \sum_n I_n \left\{\int_S \xi \frac{\epsilon^2}{\epsilon_0^2}\left[\left(\frac{\partial T_n}{e_1\partial u}\right.\right.\right.$$
$$\left. + d_n \frac{h_n^2}{k^2}\frac{\partial T_n'}{e_2\partial v}\right)\left(\frac{\partial T_m}{e_1\partial u} + d_m \frac{h_m^2}{k^2}\frac{\partial T_m'}{e_2\partial v}\right) \qquad (61)$$
$$\left. + \left(\frac{\partial T_n}{e_2\partial v} - d_n \frac{h_n^2}{k^2}\frac{\partial T_n'}{e_1\partial u}\right)\left(\frac{\partial T_m}{e_2\partial v} - d_m \frac{h_m^2}{k^2}\frac{\partial T_m}{e_1\partial u}\right)\right] dS$$
$$\left. - \int_S \xi \frac{\epsilon}{\epsilon_0}\frac{\chi_n^2\chi_m^2}{k^2} T_n T_m\, dS\right\}.$$

Similarly, we add

$$-e_3\left(\frac{\partial T_m}{e_1\partial u} + d_m \frac{\partial T_m'}{e_2\partial v}\right) \text{ times } (8)$$

and

$$-e_3\left(\frac{\partial T_m}{e_2\partial v} - d_m \frac{\partial T_m'}{e_1\partial u}\right) \text{ times } (9)$$

and integrate over the cross section:

$$\begin{aligned}\frac{dI_m}{dw} + j\omega\epsilon_0 V_m \quad = \quad & -j\omega\epsilon_0 \sum_n V_n \left\{\int_S \xi \frac{\epsilon}{\epsilon_0}\left[\left(\frac{\partial T_n}{e_1\partial u}\right.\right.\right. \\ & + d_n \left.\frac{\partial T_n'}{e_2\partial v}\right)\left(\frac{\partial T_m}{e_1\partial u} + d_m \frac{\partial T_m'}{e_2\partial v}\right) \\ & + \left.\left(\frac{\partial T_n}{e_2\partial v} - d_n \frac{\partial T_n'}{e_1\partial u}\right)\left(\frac{\partial T_m}{e_2\partial v} - d_m \frac{\partial T_m'}{e_1\partial u}\right)\right] dS \\ & \left. - \int_S \xi \frac{\epsilon}{\epsilon_0} d_n d_m \frac{\chi_n^2 \chi_m^2}{k^2} T_n' T_m' \, dS\right\}.\end{aligned} \tag{62}$$

Equations (61) and (62) are the generalized telegraphist's equations for the curved helix waveguide. The specification of the normalization factor in (60), which seemed rather arbitrary at that time, turns out in (61) and (62) to be the only right one. Only with this normalization are the mutual impedance and admittance coefficients symmetrical:

$$Y_{nm} = Y_{mn},$$
$$Z_{nm} = Z_{mn},$$

as we must expect from the symmetry properties of the curved helix waveguide structure.

Introducing travelling waves

$$\begin{aligned} V_m &= \sqrt{K_m}\,(a_m + b_m), \\ I_m &= \frac{1}{\sqrt{K_m}}\,(a_m - b_m) \end{aligned} \tag{63}$$

into (61) and (62) with $K_m = h_m/\omega\epsilon_0$, we get the more convenient form:

$$\begin{aligned} \frac{da_m}{dw} + jh_m a_m &= j \sum_n (c_{mn}^+ a_n + c_{mn}^- b_n), \\ \frac{db_m}{dw} + jh_m b_m &= -j \sum_n (c_{mn}^+ b_n + c_{mn}^- a_n). \end{aligned} \tag{64}$$

The coupling coefficients in (64) are:

$$
\begin{aligned}
c_{mn}^{\pm} = \\
&\mp \frac{k^2}{2\sqrt{h_m h_n}} \int_S \xi \frac{\epsilon^2}{\epsilon_0^2} \left[\left(\frac{\partial T_n}{e_1 \partial u} + d_n \frac{h_n^2}{k^2} \frac{\partial T_n'}{e_2 \partial v} \right) \left(\frac{\partial T_m}{e_1 \partial u} + d_m \frac{h_m^2}{k^2} \frac{\partial T_m'}{e_2 \partial v} \right) \right. \\
&\quad + \left. \left(\frac{\partial T_n}{e_2 \partial v} - d_n \frac{h_n^2}{k^2} \frac{\partial T_n'}{e_1 \partial u} \right) \left(\frac{\partial T_m}{e_2 \partial v} - d_m \frac{h_m^2}{k^2} \frac{\partial T_m'}{e_1 \partial u} \right) \right] dS \\
&\quad - \frac{1}{2} \sqrt{h_m h_n} \int_S \xi \frac{\epsilon}{\epsilon_0} \left[\left(\frac{\partial T_n}{e_1 \partial u} + d_n \frac{\partial T_n'}{e_2 \partial v} \right) \left(\frac{\partial T_m}{e_1 \partial u} + d_m \frac{\partial T_m'}{e_2 \partial v} \right) \right. \qquad (65) \\
&\quad + \left. \left(\frac{\partial T_n}{e_2 \partial v} - d_n \frac{\partial T_n'}{e_1 \partial u} \right) \left(\frac{\partial T_m}{e_2 \partial v} - d_m \frac{\partial T_m'}{e_1 \partial u} \right) \right] dS \\
&\quad \pm \frac{k^2}{2\sqrt{h_m h_n}} \int_S \xi \frac{\epsilon}{\epsilon_0} \frac{\chi_n^2 \chi_m^2}{k^2} T_n T_m \, dS \\
&\quad + \frac{1}{2} \sqrt{h_m h_n} \int_S \xi \frac{\epsilon}{\epsilon_0} d_n d_m \frac{\chi_n^2 \chi_m^2}{k^2} T_n' T_m' \, dS.
\end{aligned}
$$

We are interested here only in coupling between circular electric and other waves. Let the subscript m refer to a TE_{0m} wave. Then $J_1(k_m)$ is 0, and

$$T_m = 0, \qquad T_m' = N_m J_0(\chi_m r).$$

From (60) we get as normalization factor:

$$d_m N_m = \frac{1}{\sqrt{\pi}} \frac{k}{h_m} \frac{1}{k_m J_0(k_m)}.$$

Evaluation of (65) then yields:

$$
\begin{aligned}
c_{mn}^{\pm} &= N_n \frac{\sqrt{\pi}}{2ka} \sqrt{\frac{h_n}{h_m}} \frac{k_m k_n^2}{k_m^2 - k_n^2} J_1(k_n) \left[1 \pm \frac{h_m}{h_n} \right. \\
&\qquad + \left. \left(\frac{h_m + h_n}{h_m - h_n} \right)^{\pm 1} \frac{J_1(k_n)}{k_n J_1'(k_n)} \right] \frac{1}{R} \\
&= \frac{1}{\sqrt{2}} \sqrt{\frac{h_n}{h_m}} \frac{1}{ka} \frac{k_m k_n^2}{k_m^2 - k_n^2} \qquad (66) \\
&\quad \cdot \frac{1 \pm \dfrac{h_m}{h_n} + \left(\dfrac{h_m + h_n}{h_m - h_n} \right)^{\pm 1} Y_n}{\left[\dfrac{h_n^2}{k^2} (k_n^2 - 1) Y_n^2 + \dfrac{1}{Y_n^2} + k_n^2 \left(1 - \dfrac{1}{k^2 a^2} \right) + 2 \left(\dfrac{1}{Y_n} - Y_n \right) + \dfrac{\epsilon_e}{\epsilon_0} \dfrac{k_n^4}{k_n^{e4}} \left(2 k_n^e \cot \delta k_n^e + \dfrac{\delta k_n^{e2}}{\sin^2 \delta k_n^e} \right) \right]^{1/2}} \frac{1}{R},
\end{aligned}
$$

where

$$Y_n = \frac{J_1(k_n)}{k_n J_1'(k_n)}$$

and

$$\delta = \rho - 1.$$

With (64) and (66), the circular electric wave propagation in the curved helix waveguide can be analyzed. Neglecting backward travelling waves in (64) and considering only coupling between a circular electric wave and one other mode at a time, the coupling coefficients c_{mn}^+ and propagation constants h_n can be used in formulae like (49) and (50) to compute circular electric wave loss and mode conversion in the curved helix waveguide.

A theory of the helix waveguide, however, is complete only when the transmission and conversion properties of waves at a transition from metallic guide to helix guide is known. When we represented helix waveguide propagation in terms of normal modes of the metallic guide, we obtained these transmission and conversion properties with the matrix L in (42). To obtain the corresponding matrix in the present formulation, we express a typical normal mode of the helix waveguide in terms of normal modes of the metallic guide. To do this exactly, an infinite set of linear equations in an infinite number of unknowns would have to be solved. However, as before we may safely neglect reflected waves and match only one pair of field components. The problem is then considerably simplified, especially when we choose the longitudinal field components to be matched.

The longitudinal field components of a typical forward mode in the helix waveguide are

$$\begin{aligned} E_{zn} &= j\omega\mu \sqrt{\frac{\omega\epsilon}{h_n}} \frac{\chi_n^2}{k^2} T_n a_n , \\ H_{zn} &= j\omega\epsilon \sqrt{\frac{h_n}{\omega\epsilon}} \frac{\chi_n^2}{k^2} d_n T_n' a_n. \end{aligned} \tag{67}$$

Longitudinal field components of forward modes in the metallic waveguide are

$$\begin{aligned} E_{z(n)} &= j\omega\mu \sqrt{\frac{\omega\epsilon}{\beta_{(n)}}} \frac{\chi_{(n)}^2}{k^2} T_{(n)} a_{(n)} , \\ H_{z[n]} &= j\omega\epsilon \sqrt{\frac{\omega\mu}{\beta_{[n]}}} \frac{\chi_{[n]}^2}{k^2} T_{[n]} a_{[n]} . \end{aligned} \tag{68}$$

Matching the field components:

$$E_{zn} = \sum_n E_{z(n)}\,, \qquad H_{zn} = \sum_n H_{z[n]}$$

we can, by means of a Fourier-Bessel expansion, express the wave amplitudes of the modes in the metallic waveguide in terms of the wave amplitudes of the modes in the helix waveguide:

$$\begin{aligned} a_{(m)} &= l_{(m)n} a_n\,, \\ a_{[m]} &= l_{[m]n} a_n\,. \end{aligned} \tag{69}$$

The coefficients $l_{(m)n}$ and $l_{[m]n}$ are the elements of a matrix L which corresponds, in our present formulation, to the matrix L of (42).

To improve the approximation, we actually did not match the longitudinal field components. Rather, we obtained two slightly different sets of l's by matching first the transverse components of the electric field and then the transverse components of the magnetic field. We expect that, if we would determine a set of l's from an exact solution of the problem, the values would lie somewhere between the results of these two calculations. Since the two approximate results are near together for modes sufficiently far from cutoff, their geometric mean should furnish a still better approximation to the exact l. Typical coefficients l are thus given by:

$$\begin{aligned} l_{(m)n} &= \chi_n^{\;2} \int_S T_n T_{(m)}\, dS, \\ l_{[m]n} &= \frac{\beta_{[m]}}{k}\, \chi_n^{\;2}\, d_n \int_S T_n{}' T_{[m]}\, dS. \end{aligned} \tag{70}$$

The integrals in (70) are extended only over the part of the cross section which is inside the helix.

Calculation of the reciprocal coefficients proved the law of reciprocity $l_{n(m)} = l_{(m)n}$ and $l_{n[m]} = l_{[m]n}$ to be satisfied when the normalization factor N_n is chosen according to (60).

Evaluation of the integrals in (70) yields:

$$\begin{aligned} l_{(m)n} &= \sqrt{\epsilon_p \pi}\, N_n \frac{k_n^{\;2} J_p(k_n)}{k_n^{\;2} - k_{(pm)}^{\;2}}\,, \\ l_{[m]n} &= \frac{\sqrt{\epsilon_p \pi}\; p N_n}{\sqrt{k_{[pm]}^{\;2} - p^2}}\, \frac{\beta_{[pm]}}{k}\, \frac{k_n^{\;2} J_p(k_n)}{k_n^{\;2} - k_{[pm]}^{\;2}}\,, \end{aligned} \tag{71}$$

where the expression for N_n is given in (91) of the Appendix. There is only conversion between modes of equal azimuthal order p.

IV. MODIFIED JACKET STRUCTURES

The helix waveguide which has been analyzed in the preceding sections has a wall structure of very special and highly idealized form. Practical jackets may intentionally or unintentionally be quite different from this mathematical model. We shall discuss several modifications of the ideal shielded helix waveguide which have proven to be important in a practical helix waveguide.[7] They are either changes of the ideal structure to simplify the manufacturing process or improve the performance, or they are deviations from the ideal structure, which are unavoidable in a real structure. It turns out that, for most of these modifications, we need not work out a new theory (as in the preceding sections) but can include their effects in the foregoing formulae. A quantity which is very useful for these discussions is the wall impedance of the helix waveguide:

4.1 *The Wall Impedance of the Helix Waveguide*

In all cases of practical interest the jacket permittivity is high enough so that

$$| k_n^e | \gg | (4p^2 - 1)/8 |$$

is well satisfied and the Hankel functions may be replaced by their asymptotic expressions. The characteristic equation (58) for the normal modes of the helix waveguide then reduces to:

$$\frac{1}{k_n} \frac{J_p'(k_n)}{J_p(k_n)} - \frac{p^2 h_n^2}{k_n^3 k^2} \frac{J_p(k_n)}{J_p'(k_n)} = -\frac{\epsilon_e}{\epsilon_0} \frac{1}{k_n^e} \cot \delta k_n^e. \tag{72}$$

The right-hand side of (72) can, to the same approximation, be expressed by the impedance

$$Z = -\frac{E_{wn}}{H_{vn}} = j \frac{\chi_n^e}{\omega \epsilon_e} \tan \delta k_n^e, \tag{73}$$

which the wall presents to a typical mode of the helix waveguide:

$$\frac{1}{k_n} \frac{J_p'(k_n)}{J_p(k_n)} - \frac{p^2 h_n^2}{k_n^3 k^2} \frac{J_p(k_n)}{J_p'(k_n)} = \frac{-j}{\omega \epsilon_0 a Z}. \tag{74}$$

Thus, the separation constant k_n and with it the helix waveguide mode is determined by the wall impedance alone.

It is, on the other hand, quite easy to determine the wall impedance of a composite jacket structure to the same approximation. The physical meaning of the approximations which have been made to derive (73) is $\delta \ll 1$. The thickness of the dielectric jacket or the penetration of waves into it is small enough so that the coaxial structure can be considered plane in cartesian coordinates. Furthermore, the dependence on the azimuthal coordinate φ or v respectively is of so low an order compared to the r or u and z or w dependence that it may be neglected. The wall impedance we then calculate and quite generally use in the characteristic equation (74) is that of a symmetrical TM wave at a plane interface. For these waves the wall impedance of (73) is an exact representation of the boundary condition.

4.2 *Unshielded Helix Waveguide*

When the lossy jacket surrounding the helix is either so thick or has so high a loss factor that the electromagnetic field has died away before it reaches the metallic shield, we may remove it or substitute a different supporting structure without affecting the electrical performance of the helix waveguide. Some formulae in Section III may be simplified in this case, by letting b, the radius of the shield, go to infinity. For example, the characteristic equation (58) for the normal modes of the helix waveguide reduces to:

$$\frac{J_p'(k_n)}{J_p(k_n)} - \frac{p^2 h_n^2}{k_n^2 k^2} \frac{J_p(k_n)}{J_p'(k_n)} = \frac{\epsilon_e}{\epsilon_0} \frac{k_n}{k_n^e} \left[\frac{H_p^{(2)\prime}(k_n^e)}{H_p^{(2)}(k_n^e)} - \frac{p^2}{k_n^{e2}} \frac{h_n^2}{k_e^2} \frac{H_p^{(2)}(k_n^e)}{H_p^{(2)\prime}(k_n^e)} \right]. \quad (75)$$

Likewise, the expression (91) for the normalization factor N_n in the appendix can be somewhat simplified to give (92).

Instead of (72), the form (74) of the characteristic equation may be used; the wall impedance is in this case obtained from (73) by using the asymptotic value for the tangent function:

$$Z = \frac{\chi_n^e}{\omega \epsilon_e}. \quad (76)$$

4.3 *Dielectric Matching Layer*

The absorption of unwanted modes in the helix waveguide is critically dependent on the permittivity of the lossy jacket. In constructing a helix waveguide it is difficult to find a jacket material which has both a suitable value of complex permittivity and good enough mechanical properties to support the helix properly. A layer of lossless dielectric material in between helix and lossy jacket can serve to overcome both of these difficulties to a certain extent. By choosing a suitable material for this layer the bond between helix wires and jacket can be strengthened, thus improving the mechanical strength of the structure. Electrically, this layer acts as a radial transmission line-section. When made of the proper thickness, this transmission line transforms the wall impedance to more suitable values as far as unwanted mode attenuation is concerned.

Let Z be the input impedance of the lossy jacket as given for example by (73) or (76); then the new wall impedance in front of the dielectric layer is given by the following transformation:

$$Z' = Z_1 \frac{Z + jZ_1 \tan \chi_{n1} t}{Z_1 + jZ \tan \chi_{n1} t}. \tag{77}$$

When ϵ_1 is the permittivity of the matching layer, the radial propagation constant is

$$\chi_{n1} = \sqrt{\omega^2 \mu \epsilon_1 - h_n^2}$$

and the wave impedance is

$$Z_1 = \frac{\chi_{n1}}{\omega \epsilon_1}.$$

The expression in (77) must be substituted for the wall impedance in the characteristic equation (74).

4.4 *Laminated Jacket*

The foregoing consideration of one dielectric layer can be extended to a semi-infinite stack of laminated material having alternate thin layers of lossy and nonlossy material. It has indeed been proved very useful to have the helix jacket made of such laminations. Excellent mechanical and electrical properties have been achieved in this structure.

The wall impedance presented by a semi-infinite stack of alternating layers is found by iterating the single layer transformation of (77). This calculation has been made in a theory of laminated transmission lines:[8]

$$Z = \frac{T_{11} - T_{22}}{2T_{21}} + \frac{1}{2T_{21}} \sqrt{(T_{11} + T_{22})^2 - 4}. \tag{78}$$

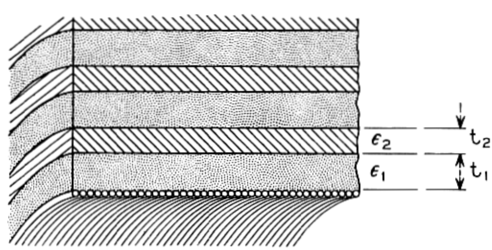

Fig. 2 — Laminated jacket of helix waveguide.

The T_{ik} are the elements of a transmission matrix relating input values of the electric and magnetic field strengths to the output values in one elementary double layer of the stack. With the constants and dimensions of Fig. 2, they are defined by

$$\begin{aligned} T_{11} &= \cos \chi_{n1}t_1 \cos \chi_{n2}t_2 - \frac{Z_1}{Z_2} \sin \chi_{n1}t_1 \sin \chi_{n2}t_2 , \\ T_{12} &= jZ_1 \sin \chi_{n1}t_1 \cos \chi_{n2}t_2 + jZ_2 \sin \chi_{n2}t_2 \cos \chi_{n1}t_1 , \\ T_{21} &= \frac{j}{Z_1} \sin \chi_{n1}t_1 \cos \chi_{n2}t_2 + \frac{j}{Z_2} \sin \chi_{n2}t_2 \cos \chi_{n1}t_1 , \\ T_{22} &= \cos \chi_{n1}t_1 \cos \chi_{n2}t_2 - \frac{Z_2}{Z_1} \sin \chi_{n1}t_1 \sin \chi_{n2}t_2 , \end{aligned} \tag{79}$$

where

$$\chi_{n1}^2 = \omega^2\mu\epsilon_1 - h_n^2,$$
$$\chi_{n2}^2 = \omega^2\mu\epsilon_2 - h_n^2$$

are the radial propagation constants in each individual layer and

$$Z_1 = \frac{\chi_{n1}}{\omega\epsilon_1},$$

$$Z_2 = \frac{\chi_{n2}}{\omega\epsilon_2},$$

are the radial wave impedances in each individual layer.

If the laminates are fine enough

$$|\chi_{n1}t_1| \ll 1,$$

$$|\chi_{n2}t_2| \ll 1,$$

the trigonometric functions may be replaced by their Taylor series. Then the wall impedance of (78) reduces to

$$Z = \frac{\chi_{nr}}{\omega\sqrt{\epsilon_z\epsilon_r}} - j\frac{1}{2}\frac{t_1t_2}{\omega\epsilon_1\epsilon_2}\frac{\omega^2\mu\epsilon_1\epsilon_2 - h_n^2(\epsilon_1 + \epsilon_2)}{\epsilon_2t_2 + \epsilon_1t_1}(\epsilon_1 - \epsilon_2). \tag{80}$$

The first term of this expression is the radial wave impedance of a homogeneous but anisotropic medium. The permittivity of this medium is, for an electric field polarized in radial direction,

$$\epsilon_r = \frac{\epsilon_1\epsilon_2(t_1 + t_1)}{\epsilon_2t_1 + \epsilon_1t_2} \tag{81}$$

and, for an electric field polarized in longitudinal or azimuthal direction,

$$\epsilon_z = \frac{\epsilon_1 t_1 + \epsilon_2 t_2}{t_1 + t_2}. \tag{82}$$

The propagation constant of this anisotropic medium in (80) is

$$\chi_{nr}^2 = \omega^2 \mu \epsilon_r - h_n^2. \tag{83}$$

The second term in (80) is a correction for the finite thickness of the laminae.

For calculating wave propagation in a helix waveguide with a laminated jacket, (78) or (80) must be substituted for the wall impedance in the characteristic equation (74).

4.5 *Finite Size of Helix Wires*

In the preceding analysis the wires of the closely wound helix had been assumed to be of so small a size that the helix could be represented by an infinitely thin sheet ideally conducting in azimuthal direction and nonconducting in longitudinal direction. This anisotropic conducting sheath, however, does not always represent the helix satisfactorily. Helices wound from the smallest feasible wire sizes — 3 to 10 mils diameter (American Wire Gauge Nos. 30 to 40) — are not completely permeable to longitudinal electric fields. Displacement currents partly bridge the gap between successive turns. By partly shielding the jacket from the helix interior, they may change the propagation characteristics substantially.

This shielding effect is most easily taken into account by a capacitance in parallel to the input impedance of the jacket. The capacitance of an infinite grating of cylindrical wires is calculated in the Appendix. With the dimensions of Fig. 3, the capacitance per square of the helix surface is given by

$$C/\text{square} = \epsilon d \left(\frac{d}{D - d} - \frac{\ln 4}{\pi} \right),$$

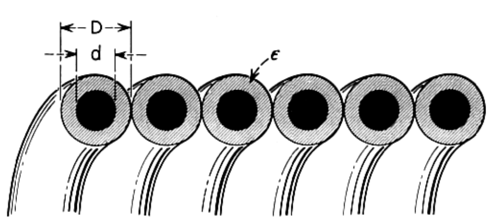

Fig. 3 — Helix wires.

where ϵ is the permittivity of the space in between wires. The corrected wall impedance is then obtained from

$$\frac{1}{Z'} = \frac{1}{Z} + j\omega\epsilon d\left(\frac{d}{D - d} - \frac{\ln 4}{\pi}\right). \tag{84}$$

Again, this expression must be substituted for the wall impedance in the characteristic equation (74).

All expressions for the wall impedance [(73), (76), (77), (78), (80), (84)] contain implicitly the axial propagation constant jh_n of the particular mode under consideration, and it is only through the characteristic equation (74) that this propagation constant will be determined.

In Section II, on the other hand, where the helix waveguide propagation is expressed in terms of normal modes of the solid wall guide, the wall impedance as introduced in the boundary condition (18) is not associated with a particular mode. The propagation constant jh_n remains undetermined. The boundary condition (18) cannot exactly replace a complex jacket structure.

For all cases, however, in which the modes under consideration are far from cutoff, the propagation constants are nearly equal to that of free space. We may then replace h_n by $\omega\sqrt{\mu_0\epsilon_0}$ in all expressions for the wall impedance and use them in (18) and the corresponding equations.

V. APPLICATIONS

Three different applications of the helix waveguide for circular electric wave transmission have been mentioned in the introduction. The formulae of the preceding sections will now be used to calculate the transmission properties of helix waveguide in the different applications. The theoretical values will be compared with results of measurements.

5.1 *Helix Waveguide Mode Filter*

It has been shown both theoretically and experimentally that the transmission characteristic of the circular waveguide can be substantially improved by the insertion of mode filters at intervals along the waveguide.[9] Conversion of energy to unwanted modes and reconversion at any imperfections of the waveguide seriously disturb the TE_{01} transmission characteristic. Mode filters, which provide low loss for the TE_{01} mode and high loss for all unwanted modes, greatly reduce the effects of mode conversion-reconversion by dissipating most of the converted power in unwanted modes before reconversion.

Helix waveguide has the desired properties of low TE_{0n} attenuation and high loss for all other modes. It therefore is well suited for a mode filter. To design a helix waveguide mode filter one would choose a lossy material for the jacket which maximizes the attenuation constants of the unwanted modes of propagation. A detailed analysis[2] of the helix waveguide modes has shown, however, that there is no unique solution to this problem. As one changes the complex permittivity of the jacket, the attenuation constants of some modes increase while those of others decrease after passing through a maximum. Furthermore, a normal mode of a metallic waveguide incident in a helix waveguide will scatter its power into quite a few modes of the helix waveguide. As a result, a helix waveguide section inserted into a metallic waveguide will not only dissipate power in unwanted modes but will also introduce cross-coupling between unwanted modes. To find the transmission and conversion properties of a helix waveguide in the arrangement of Fig. 4 the matrix L of (42), as a scattering matrix between metallic waveguide modes and helix waveguide modes, must be combined with the transmission matrix T of the helix waveguide to give the relation between mode amplitudes at the input A_i and output A_0 :

$$A_0 = LTL_tA_i , \tag{85}$$

where T is a diagonal matrix, the elements of which are transmission coefficients of the helix waveguide modes

$$t_{nn} = e^{-jh_nz}. \tag{86}$$

Equation (85) has been evaluated for a typical helix waveguide with a relative permittivity $\epsilon/\epsilon_0 = 4 - j1$, and an inner radius to wavelength ratio $a/\lambda = 4.70$. This evaluation was extended over the TE_{11} , TM_{11} and TE_{12} modes of the metallic waveguide, and it was sufficient to take only five modes (TE_{11} , TE_{12} , TM_{12} , TE_{13} and TM_{13}) of the helix waveguide into account. The propagation constants jh_n of these helix waveguide modes were taken from the previously cited analysis of the helix waveguide.[2] For the elements of L, expressions (71) were substituted. The resulting transmission loss and conversion loss curves are shown in Fig. 5(a).

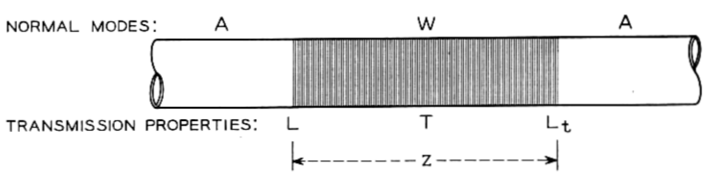

Fig. 4 — Matrices of mode filter.

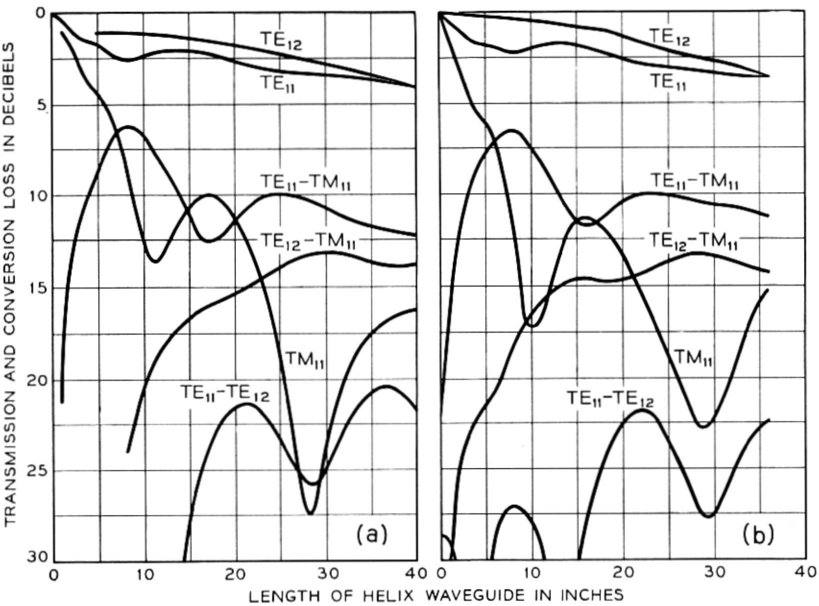

Fig. 5 — (a) Calculated transmission and conversion loss in helix waveguide: $a/\lambda = 4.70$, semi-infinite jacket with $\epsilon/\epsilon_0 = 4 - j1$; (b) measured transmission and conversion loss in helix waveguide of Fig. 6, $f = 55.5$ kmc.

The results of measurements on an 18 in. long section of 2 in. I.D. helix waveguide are shown in Fig. 5(b). This measured waveguide section has the helix wire dimensions and a jacket structure as shown in Fig. 6. The values of anisotropic permittivity of the laminated lossy material have been determined separately by impedance measurements on small samples in RG-98/U waveguide. The radial impedance of this laminated material is given by the first term in (80). The layer of glass roving between the lossy laminate and the helix wires transforms this impedance according to (77). Finally, the capacitance between helix wires changes the radial impedance according to (84). The resulting wall impedance is $Z = (147 + j22)\Omega$. The mathematical model of a helix waveguide which was used to calculate the curves of Fig. 5(a) has an isotropic and homogeneous jacket of relative permittivity $\epsilon/\epsilon_0 = 4 - j1$. Its wall impedance as calculated from (76) is $Z = (162 + j14)\Omega$. Comparing both wall impedances we find that the measured helix waveguide of Figs. 5(b) and 6 and the mathematical model of Fig. 5(a) are nearly equivalent. Thus the calculated curves of Fig. 5(a) may be compared

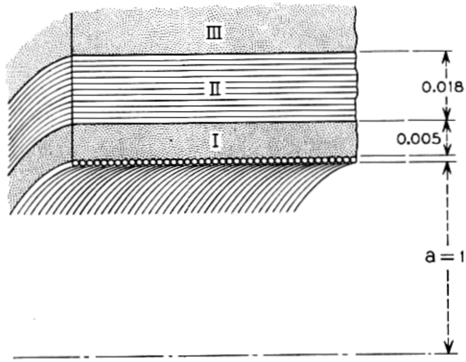

Fig. 6 — Helix waveguide structure. Helix: No. 37 copper wire with heavy Formex coat; Mediums I and III: Fiberglas laminated with epoxy resin; Medium II: six layers of tin oxide-coated glass cloth; $\epsilon_z/\epsilon_0 = 9 - j13$, $\epsilon_r/\epsilon_0 = 5 - j1$ at 55.5 kmc.

to the measured curves of Fig. 5(b). We find indeed very good agreement.

The transmission and conversion loss of the various modes were measured with millimeter-wave short pulse test equipment,[10] using the arrangement shown in Fig. 7. The pulses had a base width of about 3 millimicroseconds. Mode discrimination in the mode couplers and mode transducers combined with time discrimination based on the different group velocities of modes in the 220 ft. long waveguide provided sufficient over-all discrimination to identify energy travelling in different modes.

The results of Fig. 5 do not give an answer for designing helix waveguide for mode filtering purposes. They do, however, give assurance that the theory gives correct results even for quite complicated jacket structures, and that this theory may safely be used to design helix waveguide mode filters.

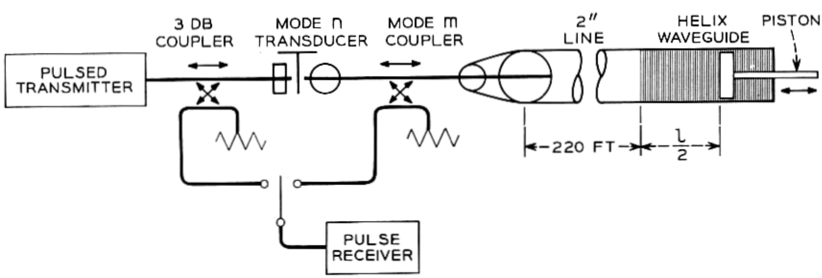

Fig. 7 — Measurement of transmission and conversion loss in helix waveguide.

The high amount of mode conversion which is caused by a helix waveguide of a certain length is perhaps surprising. The mode conversion loss between TE_{11} and TM_{11} is as low as 6 db in the case treated above. There may be cases in which this high mode conversion is undesirable. In order to reduce it, the abrupt transition from solid waveguide to helix waveguide may be replaced by a taper in wall impedance. The formulae of Section II give the basis to analyze such a wall impedance taper. The generalized telegraphist's equations in this section must then be solved for varying coupling coefficients instead of constant coupling coefficients.

5.2 *Intentional Bends in Helix Waveguide*

The analysis of a tapered curvature bend[3] has shown that the circular electric wave can be transmitted around bends with very low losses in a waveguide in which the degeneracy of equal phase velocity between TE_{01} and TM_{11} is broken up by lossless means. The shielded helix waveguide having a low-loss dielectric between the helix and the highly conducting metallic shield lends itself perfectly to this application.

A curvature taper on both sides of the bend serves to transform the normal mode of the straight pipe into the normal mode of the curved region and *vice versa*. A practical form for a tapered curvature bend is shown in Fig. 8; the region of constant curvature has vanished and all that remains is a triangular curvature distribution. This curvature dis-

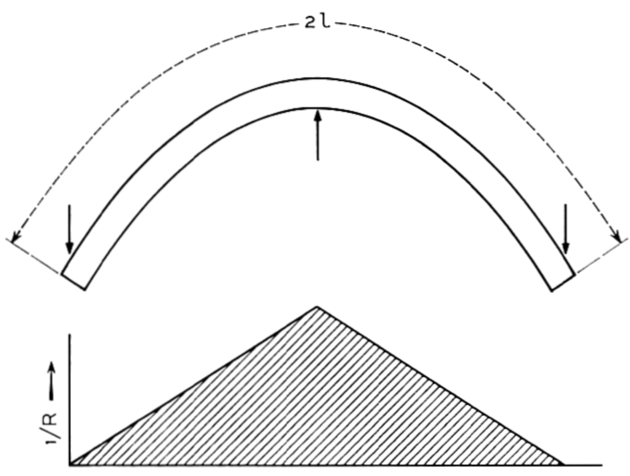

Fig. 8 — Triangular curvature distribution of an elastic deflection.

tribution can easily be made by bending the waveguide elastically over a fixed center support with forces acting on both ends.

The residual mode conversion in such a triangular curvature distribution is calculated by solving the coupled line equations for linearly varying coupling coefficients with suitable approximations for gentle curvature. Thus, at the end of a linear curvature taper of length l each mode n coupled to TE_{01} through curvature causes a mode conversion loss of

$$A_{cn} = \mathrm{Re}\left[\frac{c_{0n}^{\;2}}{\Delta\gamma_n^{\,4} l^2}\left(1 - e^{-\Delta\gamma_n l} - \Delta\gamma_n l\right)\right] \text{ nepers,} \tag{87}$$

where c_{0n} is the coefficient of curvature coupling (66) between TE_{01} and a coupled mode n at the point of maximum curvature, and $\Delta\gamma_n$ is the difference in propagation-constant between the coupled mode n and TE_{01}.

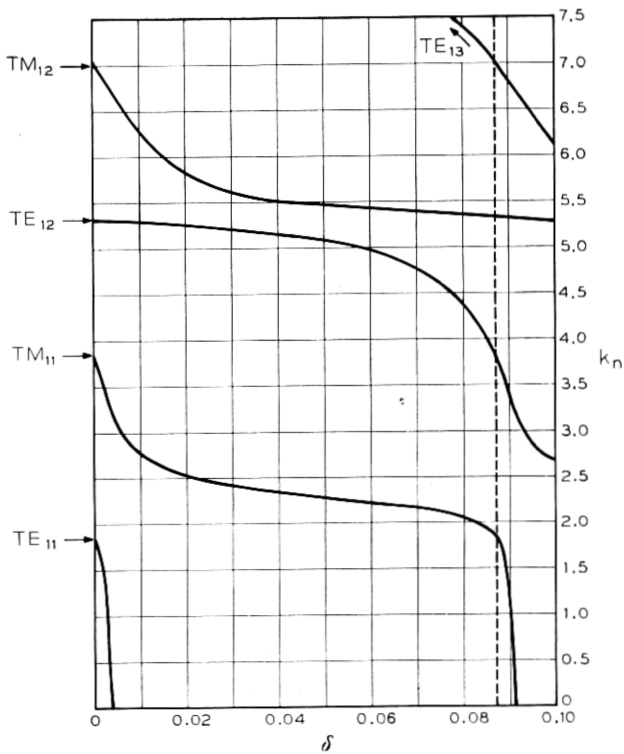

Fig. 9 — Solution of characteristic equation for shielded helix waveguide with lossless jacket; $\epsilon/\epsilon_0 = 2.5$, $a/\lambda = 4.70$.

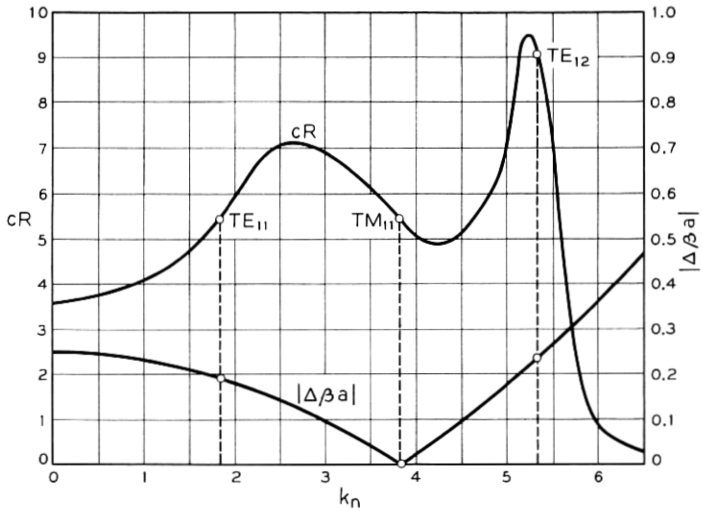

Fig. 10 — Difference in phase constant and coefficient of curvature coupling to TE_{01} in shielded helix waveguide; $a/\lambda = 4.70$.

The TE_{01} mode of the straight waveguide in passing through the curvature taper is transformed to the local normal mode of the curved region. It suffers a slight change in field configuration and consequently a change in attenuation constant. Thus, in a linear curvature taper of length l each mode coupled to TE_{01} by curvature causes an additional normal mode loss of

$$A_{bn} = \mathrm{Re}\left[\frac{c_{0n}^{\,2} l}{3\Delta\gamma_n}\right] \text{nepers.} \tag{88}$$

There is another way to calculate this normal mode loss: D. Marcuse has solved the boundary problem of the curved helix waveguide directly for the TE_{01} wave.[11] He obtains a closed expression for the curvature attenuation, which is in most cases easier to evaluate than a sum of the terms given by (88).

To provide data for the design of a low-loss helix waveguide for intentional bends, several of the expressions in Section III have been evaluated. In Fig. 9 the solution of the characteristic equation (72) is plotted in the range of interest for $p = 1$. A relative permittivity of 2.5 is a typical value for low loss dielectric materials. The ratio $a/\lambda = 4.70$ corresponds to a 2 in. I.D. helix waveguide operated at 55.5 kmc. In Fig. 10 the coefficient of curvature coupling from (66) and the difference in phase constant have been plotted for this helix waveguide. The mode

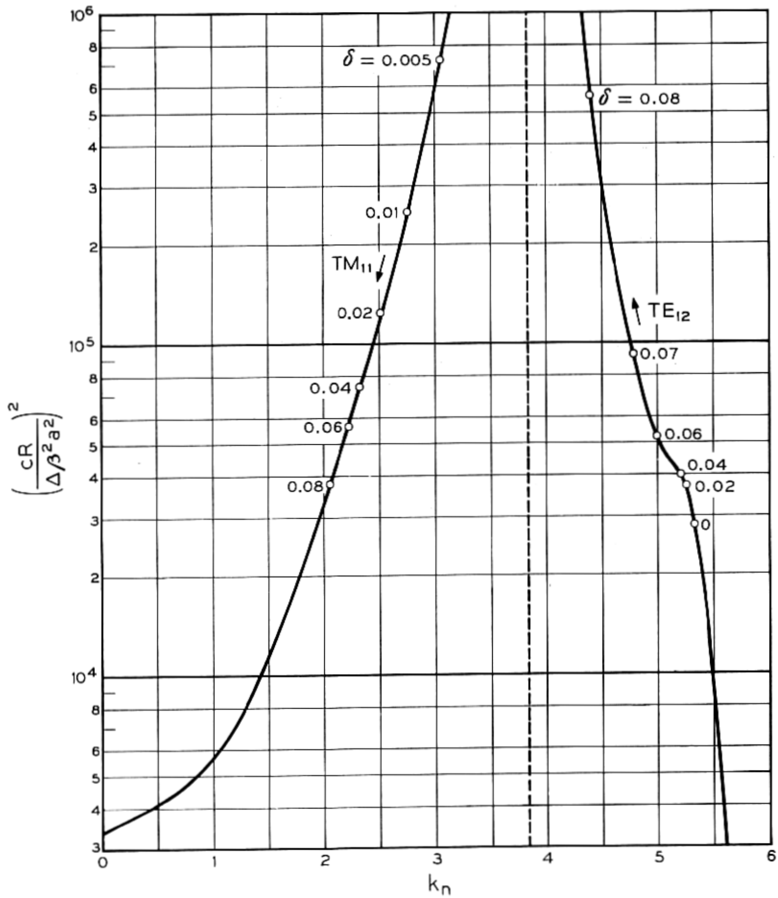

Fig. 11 — Factor of mode conversion loss in linear curvature taper of shielded helix waveguide; $\epsilon/\epsilon_0 = 2.5$, $a/\lambda = 4.70$.

conversion factor shown in Fig. 11 is found by combining the two curves of Fig. 10. This factor facilitates the calculation of mode conversion in the tapered curvature bend of Fig. 8.

An inspection of these conversion loss figures as well as of D. Marcuse's normal mode loss figures shows that, for optimum performance in a tapered curvature bend, the distance between helix and shield should be about a quarter of the radial wavelength in the jacket material. In no case should this distance approach a half radial wavelength anywhere in the frequency range.

Shielded helix waveguide with a low-loss jacket has been made with materials and construction techniques presently available in Bell Telephone Laboratories. The details of this waveguide are shown in Fig. 12. The TE_{01} loss in this structure was measured by a resonant cavity method both for the straight guide and the guide bent to various curves between 0 and 4.2 degrees. The curvature distribution was that of Fig. 8. Reasonable agreement between measured and calculated values of curvature loss was found. The measured loss followed closely the square-law dependence on curvature. At a total bending angle of 4.2 degrees the additional curvature loss in the 9 ft. long curved section was measured at 55.5 kmc to be 0.004 db. This figure is nearly equivalent to doubling the length of the waveguide. Mode filters on both sides of the curved section presented enough dissipation to avoid spurious mode interference in the measurements.

5.3 *All-Helix Waveguide*

A third and probably the most important application is a transmission line entirely consisting of helix waveguide. Present experimental experience shows that an all-helix waveguide line must present enough loss to unwanted modes so that power in these modes is dissipated at the same rate as it is converted at imperfections of the waveguide. In addition, the jacket of the helix waveguide should be designed so as to minimize the circular electric wave losses in bends, allowing relaxation of the straightness tolerances. Obviously, these two requirements contradict each other to a certain extent. A compromise will have to be chosen

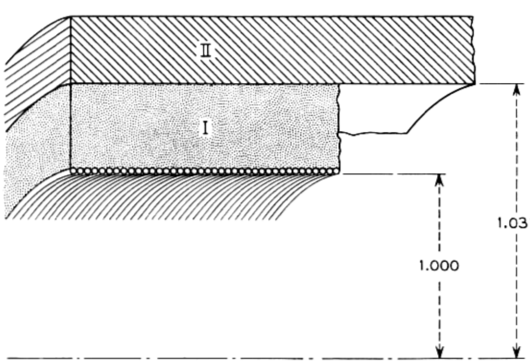

Fig. 12 — Shielded helix waveguide with low loss jacket. Helix: No. 37 copper wire with heavy Formex coat; Medium I: glass cloth laminated with epoxy resin, $\epsilon/\epsilon_0 = 4 - j0.1$ at 55.5 kmc; Medium II: copper tubing.

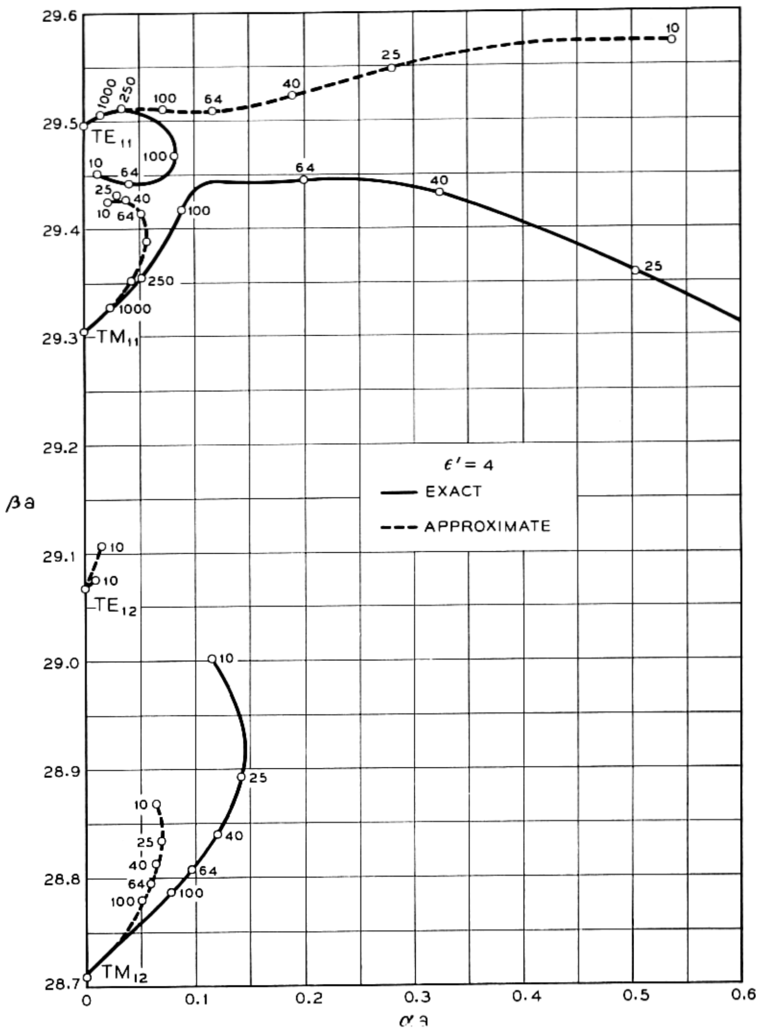

Fig. 13 — Propagation constants in helix waveguide; $a/\lambda = 4.70$, $\epsilon' = 4$. Representative values of ϵ'' are shown on the curves.

between sufficiently high unwanted mode loss and sufficiently low TE_{01} curvature loss. This compromise will be made on the basis of tolerances. While the manufacturing tolerances call for a mode-filtering helix waveguide, the laying tolerances call for low TE_{01} loss in random curvature.

However, it is to be expected that, as the art of making helix waveguide is improved and imperfections can be controlled better, the requirement of low curvature loss will become more important and less unwanted mode loss can be tolerated.

The first information needed for the design of a helix waveguide in this application is the unwanted mode loss. It is contained in a detailed analysis of the unwanted mode propagation in helix waveguide.[2] Some of the results are taken from this analysis and plotted in Figs. 13 and 14.

Also plotted in Figs. 13 and 14 are the approximate values of the

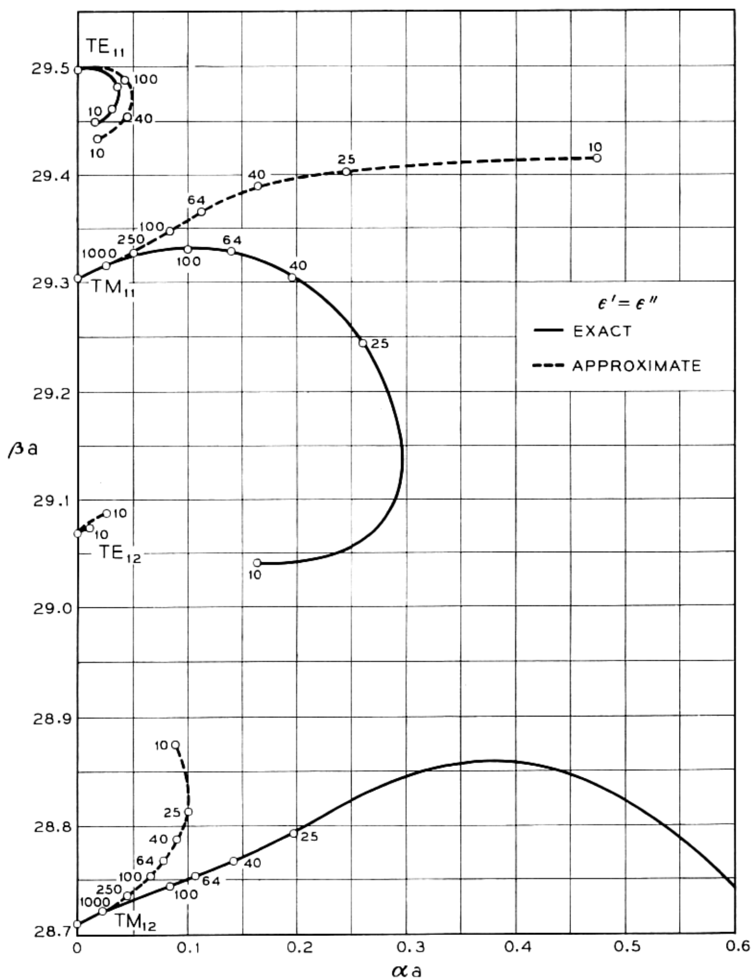

Fig. 14 — Propagation constants in helix waveguide; $a/\lambda = 4.70$, $\epsilon' = \epsilon''$. Representative values of ϵ'' are shown on the curves.

propagation constants which have been obtained as solutions of the characteristic equation (44) in Section II. The characteristic equation (44) has been reduced to a quartic equation by taking only four modes of the metallic guide (TE_{11}, TM_{11}, TE_{12}, TM_{12}) into account to represent the lower order modes with $p = 1$ in the helix waveguide. From Figs. 13 and 14 it has to be concluded that this representation is obviously a very poor one. At still fairly high values of the jacket permittivity, there is already a marked deviation of the approximate values from the exact curves. For a better representation in this large waveguide size, many more modes of the metallic guide have to be taken into account. It is therefore more convenient in most helix waveguide problems to use the representation of Section III with modes of the helix waveguide rather than the representation of Section II with modes of the metallic guide.

Imperfections like tilts and offsets or changes in diameter in an otherwise ideal guide convert TE_{01} power to unwanted modes. The effect of most of these imperfections in metallic waveguide has been analyzed in detail by S. P. Morgan, Jr., as quoted elsewhere.[1] More recently, another analysis has been made.[12]

For the helix waveguide the results of this analysis can be combined with the scattering matrix L of (42) to give the conversion from TE_{01} to the unwanted modes in the helix waveguide at these imperfections. Thus, given a certain distribution of imperfections in a helix waveguide, mode conversion and reconversion effects can be calculated. From such calculations the required unwanted mode loss to reduce the degrading effects of imperfections on TE_{01} propagation to an acceptable degree can be found.

The second requirement for an all-helix waveguide is low TE_{01} curvature loss. To find the TE_{01} curvature loss the expressions (47) or (66) for the coefficient of curvature coupling can be evaluated. The results of such an evaluation are plotted in Figs. 15 and 16. Here again the approximation (47) with only four modes (TE_{11}, TM_{11}, TE_{12}, TM_{12}) of the metallic guide deviates markedly from the exact values according to (66) for a low permittivity of the jacket.

Note that in the curved helix waveguide the TE_{01}-wave couples to all TM_{1n} and TE_{1n} waves. In the curved metallic waveguide the TE_{01} couples to all TE_{1n} but only to TM_{11}.

With the coupling coefficients on hand, TE_{01} loss and mode conversion can be calculated with formulae like (49) and (50). The perturbation of the TE_{01} propagation constant in (49), especially, means an increase α_c of TE_{01} attenuation. In Fig. 17 this attenuation increase α_c has been

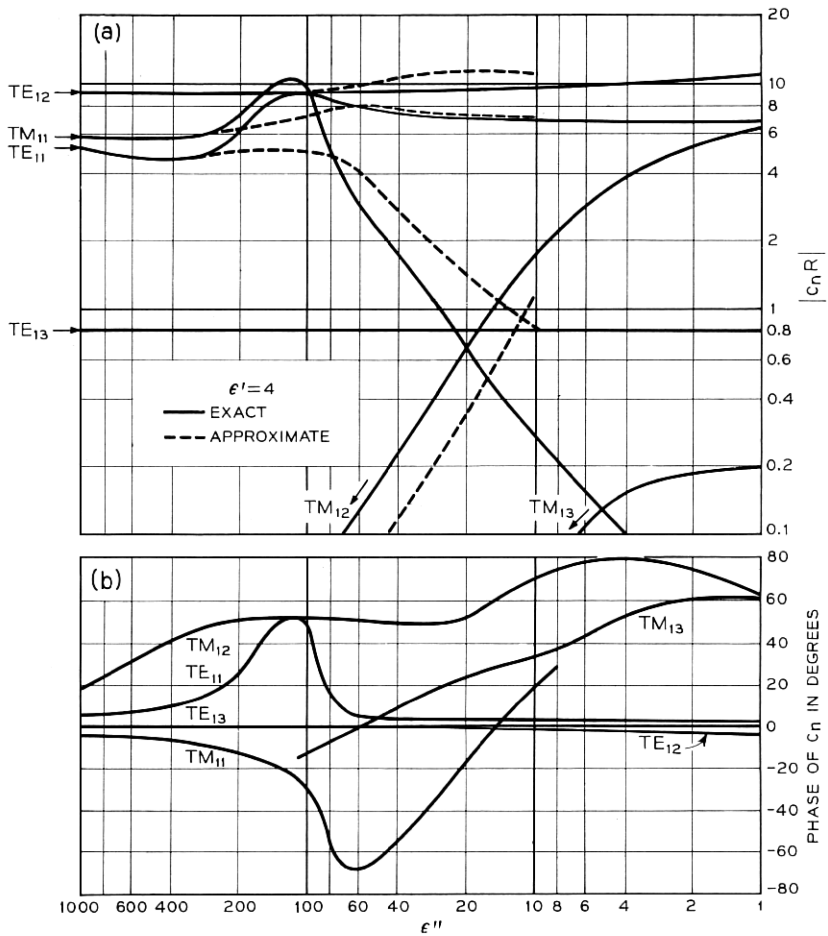

Fig. 15 — Coupling coefficient between TE_{01} and unwanted modes in curved helix waveguide; $a/\lambda = 4.70$, $\epsilon' = 4$.

plotted in a reduced form. The approximate values have again been obtained from the representation of Section II taking only four modes (TE_{11}, TM_{11}, TE_{12}, TM_{12}) into account. They deviate substantially from the exact values as obtained from Section III and equation (66). As mentioned earlier, α_c can also and more conveniently be calculated from D. Marcuse's normal mode solution of the curved helix waveguide.[11] Values for α_c of that calculation coincide with the exact curves of Fig. 17.

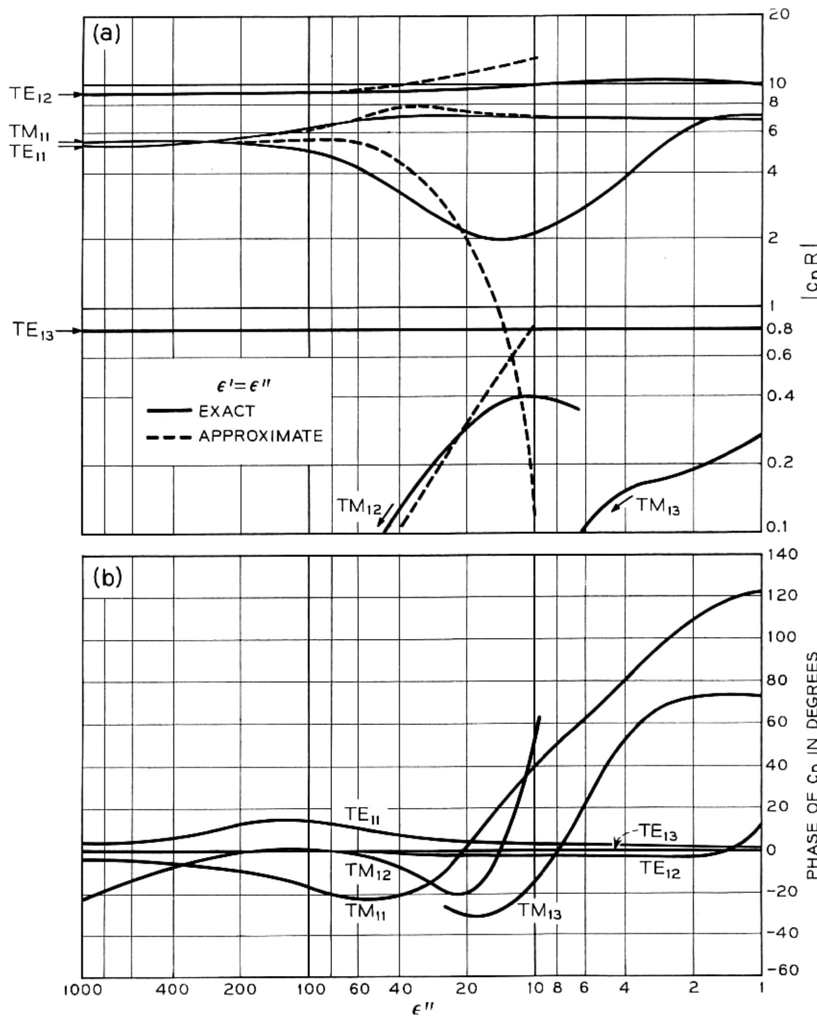

Fig. 16 — Coupling coefficient between TE_{01} and unwanted modes in curved helix waveguide; $a/\lambda = 4.70$, $\epsilon' = \epsilon''$.

The mode conversion which occurs in regions of changing curvature can be calculated from (50) if the change in curvature is abrupt, or from a solution of the coupled line equations with changing coupling coefficients when the curvature is changing gradually. Because of the laws of elasticity, the most common kind of curvature change, either intentionally or unintentional, is the linear curvature taper. The mode conversion loss in a linear curvature taper is given by (87). From this expression it can be estimated if mode conversion effects in a changing curvature are large enough to influence the design of a helix waveguide. Usually it is found that this mode conversion is small enough to be neglected and that only the curvature attenuation α_c must be made as small as possible to optimize the performance of an all-helix waveguide in bends.

Here again, as in the case of the shielded helix waveguide with a lossless jacket, a certain distance between helix wires and shield minimizes the curvature attenuation. The distance should be about a quarter of the radial wavelength in the jacket material. It should approach half of this wavelength nowhere in the frequency range.

Measurements of TE_{01} attenuation in bends have been made in the two different helix waveguides shown in Fig. 18. Eight-foot-long sections of the waveguides were bent elastically to the triangular curvature distribution of Fig. 8. The average curvature of this distribution is found by taking the square-law dependence between loss and curvature into account. The TE_{01} transmission loss was measured with a resonant cavity method for varying degrees of curvature. In the lossless helix waveguide, for intentional bends the TE_{01} transmission loss is composed of normal mode attenuation and mode conversion loss. However, in the present test of the lossy helix waveguide mode conversion losses can be neglected as compared to normal mode attenuation. The measured in-

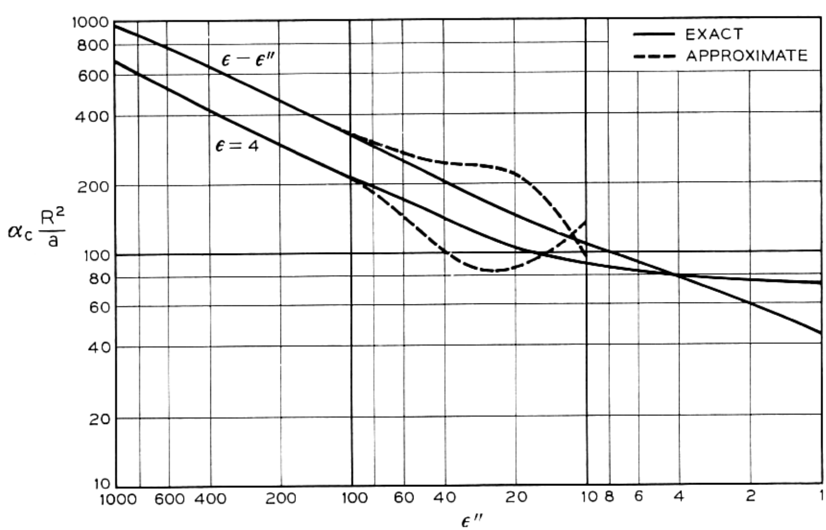

Fig. 17 — Increase of TE_{01} attenuation in curved helix waveguide; $a/\lambda = 4.70$.

crease in TE_{01} transmission loss in the curved waveguide can therefore be interpreted as additional TE_{01} attenuation per unit length. The results follow closely the square-law dependence on curvature and agree with theoretical values. The lower value of curvature attenuation in the second helix waveguide doubles the theoretical TE_{01} attenuation at a radius of curvature of 320 ft.

VI. CONCLUSIONS

Circular electric wave loss, mode conversion and unwanted mode loss can be calculated from generalized telegraphist's equations for the curved helix waveguide. A wall impedance can be used to represent the boundary condition at the helix interface. The effect of a composite jacket structure and of finite size helix wires can be taken into account in this wall impedance.

Three different applications of shielded helix waveguide for circular electric wave transmission require different designs for optimum performance. Helix waveguide as mode filter should have a highly lossy jacket between helix and shield for high unwanted mode absorption. An all-helix waveguide transmission line should have a medium lossy jacket to reduce TE_{01} loss in gentle bends and still maintain sufficient unwanted

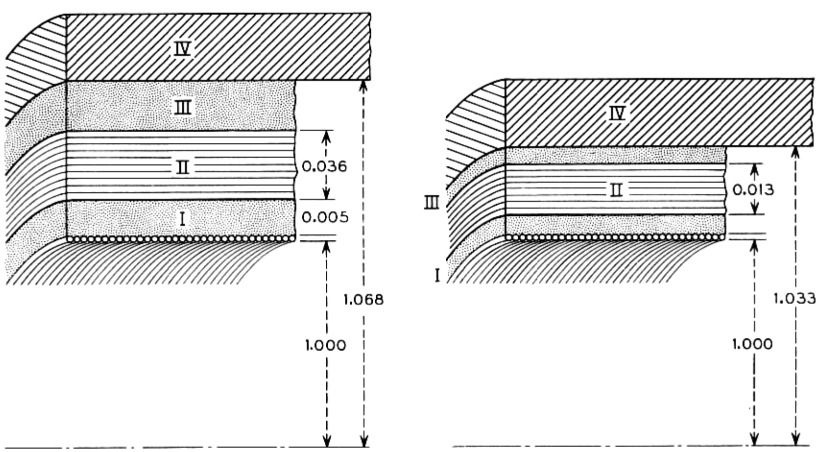

Fig. 18 — Shielded helix waveguide with lossy jacket. Helix: No. 37 copper wire with heavy Formex coat; Mediums I and III: glass cloth laminated with epoxy resin; Medium II: carbon loaded paper laminated with epoxy resin, (left) $\epsilon_z/\epsilon_0 = 15 - j14$, $\epsilon_r/\epsilon_0 = 9 - j2$; (right) $\epsilon_z/\epsilon_0 = 4.7 - j2.1$, $\epsilon_r/\epsilon_0 = 3.9 - 0.6$ at 55.5 kmc, Medium IV: steel tubing. TE_{01} curvature loss $\alpha_c(R^2/a)$ at 55.5 kmc: (left) measured, 79, calculated, 84; (right) measured, 48, calculated, 40.

mode absorption. For sharp intentional bends, the material between helix and shield should have low losses and the shield should be highly conducting. In all three applications the optimum distance between helix and shield is a quarter of the radial wavelength in the jacket material.

VII. ACKNOWLEDGMENT

The numerical evaluations which are plotted in Figs. 5, 13, 14, 15, 16 and 17 were programmed by Mrs. C. L. Beattie for automatic execution on an IBM 650 magnetic drum calculator. Measurements of TE_{01} loss were made with high-Q test equipment developed by J. A. Young. Short pulse tests were made with equipment developed by C. A. Burrus. C. F. P. Rose oversaw the construction of helix waveguides that have been tested. J. W. Bell and G. D. Mandeville assisted during the measurements. For a helpful discussion the writer is indebted to S. A. Schelkunoff.

APPENDIX

Normalization of Modes in Helix Waveguide

The orthogonality relation (60) for $n \neq m$ has been proven for exponential modes on an inhomogeneous cylindrical structure bounded by opaque walls or unbounded.[13]

The right-hand side of (60) can be rewritten as

$$\frac{1}{V_n I_m} \int_S (E_{tn} \times H_{tm})\, dS$$

$$= \int_S \frac{\epsilon}{\epsilon_0} \Big[(\text{grad } T_n)(\text{grad } T_m) + d_n d_m (\text{grad } T_n')(\text{grad } T_m') \tag{89}$$

$$- d_m \frac{h_m^2}{k^2} (\text{flux } T_n)(\text{grad } T_m') + d_n (\text{flux } T_n')(\text{grad } T_m) \Big]\, dS.$$

Partial integrations, like Green's theorem,

$$\int_S (\text{grad } T_n)(\text{grad } T_m)\, dS = \int_v T_m \frac{\partial T_n}{e_1 \partial u} e_2\, dv + \int_S \chi_n^2 T_n T_m\, dS,$$

and

$$\int_S (\text{flux } T_n)(\text{grad } T_m)\, dS = -\int_v T_n \frac{\partial T_m}{e_2 \partial v} e_2\, dv = \int_v T_m \frac{\partial T_n}{e_2 \partial v} e_2\, dv$$

reduce (89) to:

$$\int_S \frac{\epsilon}{\epsilon_0} \chi_n^2 \left(T_n T_m + d_n d_m \frac{h_m^2}{k^2} T_n' T_m' \right) dS + \int_v \frac{\epsilon}{\epsilon_0} T_m \left[\frac{\partial T_n}{e_1 \partial u} + d_n \frac{\partial T_n'}{e_2 \partial v} \right] e_2 \, dv - \int_v \frac{\epsilon}{\epsilon_0} d_m \frac{h_m^2}{k^2} T_m' \left[\frac{\partial T_n}{e_2 \partial v} - d_n \frac{\partial T_n'}{e_1 \partial u} \right] e_2 \, dv.$$

The integrand of the last term is continuous across the helix boundary and vanishes at the shield. It therefore cancels out;

$$\frac{1}{V_n I_m} \int (E_{tn} \times H_{tm}) \, dS = \int_S \frac{\epsilon}{\epsilon_0} \chi_n^2 \left(T_n T_m + d_n d_m \frac{h_m^2}{k^2} T_n' T_m' \right) dS + \int_v \frac{\epsilon}{\epsilon_0} T_m \left(\frac{\partial T_n}{e_1 \partial u} + d_n \frac{\partial T_n'}{e_2 \partial v} \right) e_2 \, dv. \tag{90}$$

From (90) the orthogonality relation can be verified for $n \neq m$.

To calculate the normalization factor N_n we substitute (51) for the T functions in (90) and perform the integrations. Since in all cases of practical interest $| k_n^e | \gg | (4p^2 - 1)/8 |$, the Hankel functions may be replaced by their asymptotic expressions. Then, in order to satisfy (60) the normalization factor has to be

$$N_n = \frac{\sqrt{2}}{\sqrt{\pi} \, J_p(k_n)} \left[\frac{h_n^2}{k^2} p^2 (k_n^2 - p^2) Y_n^2 + \frac{1}{Y_n^2} + k_n^2 \left(1 - \frac{p^2}{k^2 a^2} \right) + 2 \left(\frac{1}{Y_n} - p^2 Y_n \right) + \frac{\epsilon_e}{\epsilon_0} \frac{k_n^4}{k_n^{e3}} \left(2 \cot \delta k_n^e + \frac{\delta k_n^e}{\sin^2 \delta k_n^e} \right) \right]^{-1/2}, \tag{91}$$

where

$$Y_n = \frac{J_p(k_n)}{k_n J_p'(k_n)}.$$

For the unshielded helix waveguide described in Section IV the normalization factor is given by:

$$N_n = \frac{\sqrt{2}}{\sqrt{\pi} \, J_p(k_n)} \left[\frac{h_n^2}{k^2} p^2 (k_n^2 - p^2) Y_n^2 + \frac{1}{Y_n^2} + k_n^2 \left(1 - \frac{p^2}{k^2 a^2} \right) + 2 \left(\frac{1}{Y_n} - p^2 Y_n \right) + j2 \frac{\epsilon_e}{\epsilon_0} \frac{k_n^4}{k_n^{e3}} \right]^{-1/2}. \tag{92}$$

For the other jacket structures it is not an easy matter to calculate the normalization factor. Finding the field vectors in the jacket region and integrating over the cross-product of the transverse components is quite involved, even when asymptotic approximations such as in (91) are substituted. A further approximation, however, eliminates this problem. The integral on the left-hand side of (89) is the flux of the Poynting vector, through a waveguide cross section. From the dimensions of the helix waveguide we may safely conclude that for a typical mode the power flowing in the jacket is small compared to the power flowing inside of the helix in all cases of practical interest. Then we may extend the integral in (89) only over the helix interior and neglect the last terms under the square root of (91) or (92).

Capacitance of Plane Grating of Cylindrical Wires

The contour in the z-plane of Fig. 19 is an elementary cell of the field surrounding a plane grating of cylindrical wires. Its transformation to the strip $0 \leqq u \leqq \pi$ of the w-plane is approximately effected by[14]

$$z = \frac{D}{\pi(1 + \nu)} \left[\tanh^{-1} \sqrt{\frac{z_1 - 1}{z_1 + a}} + \nu \tanh^{-1} \sqrt{\frac{z_1 + 1}{z_1 + a}} \right] \qquad (93)$$

and

$$z_1 = \frac{a - 1}{2} \cos w - \frac{a + 1}{2}, \qquad (94)$$

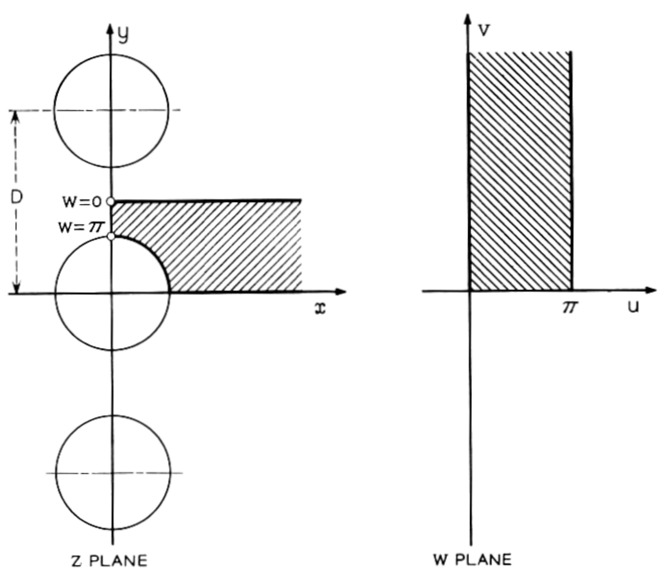

Fig. 19 — Conformal mapping of wire grating.

where ν is the root of

$$\coth^2\left(\frac{\pi}{c}\frac{d}{D}\frac{1+\nu}{\nu}\right) - \cot^2\frac{\pi}{2}\frac{d}{D}(1+\nu) = 1 \tag{95}$$

and a is given by

$$a = 1 + 2\cot^2\frac{\pi}{2}\frac{d}{D}(1+\nu). \tag{96}$$

A uniform electric field polarized in the direction of the y-axis is fringed by the grating. The capacitance of this fringing field is the difference between the capacitance of the z-plane contour and a parallel plate condenser of plate distance $D/2$ and extension $2x$:

$$\frac{C}{\epsilon} = \lim_{x\to\infty}\left(\frac{2}{\pi}v - \frac{4x}{D}\right). \tag{97}$$

Substituting for v from (93) and (94) we get, instead of (97),

$$\frac{C}{\epsilon} = \frac{2}{\pi}\left[\frac{\ln(a+1) + \nu\ln(a-1)}{1+\nu} - \ln(a-1)\right]. \tag{98}$$

For $D/d = 1$ the root of (95) is $\nu = 0$. When d is only slightly smaller than D, as is the case in a closely wound helix, ν is small and the argument of the cot in (95) is nearly $\pi/2$, while the argument of the coth is very large. Then, with

$$\frac{d}{D}(1+\nu) = (1+\eta)$$

the cot and coth functions can be approximated by:

$$\cot\frac{\pi}{2}\frac{d}{D}(1-\nu) = \frac{\pi}{2}\eta,$$

$$\coth\frac{\pi}{2}\frac{d}{D}\frac{(1+\nu)}{\nu} = 1 + 2e^{-\pi}\frac{d}{D-d}.$$

Instead of (95) we get

$$\frac{\pi^2}{4}\eta^2 = 4e^{-\pi}\frac{d}{D-d}.$$

Substituting for a from (96) into (98), the capacitance is

$$\frac{C}{\epsilon} = 2\frac{d}{D}\left(\frac{d}{D-d} - \frac{\ln 4}{\pi}\right). \tag{99}$$

REFERENCES

1. Miller, S. E., Waveguide as a Communication Medium, B.S.T.J., **33,** Nov. 1954, pp. 1209–1265.
2. Morgan, S. P. and Young, J. A., Helix Waveguide, B.S.T.J., **35,** Nov. 1956, pp. 1347–1384.
3. Unger, H. G., Normal Mode Bends for Circular Electric Waves, B.S.T.J., **36,** Sept. 1957, pp. 1292–1307.
4. Schelkunoff, S. A., Conversion of Maxwell's Equations into Generalized Telegraphist's Equations, B.S.T.J., **34,** Sept. 1955, pp. 995–1043.
5. Morgan, S. P., Theory of Curved Circular Waveguide Containing an Inhomogeneous Dielectric, B.S.T.J., **36,** Sept. 1957, pp. 1209–1251.
6. Guillemin, E. A., *The Mathematics of Circuit Analysis*, John Wiley & Sons, New York, 1950, pp. 111–122.
7. Rose, C. F. P., Research Models of Helix Waveguide, B.S.T.J., **37,** May 1958, pp. 679–688.
8. Morgan, S. P., Mathematical Theory of Laminated Transmission Lines, B.S.T.J., **31,** September 1952, pp. 883–949.
9. Warters, W. D., The Effects of Mode Filters on the Transmission Characteristics of Circular Electric Waves in a Circular Waveguide, B.S.T.J., **37,** May 1958, pp. 657–677.
10. Burrus, C. A., Millimicrosecond Pulses in the Millimeter Wave Region, Rev. Sci. Instr., **28,** Dec. 1957, pp. 1062–1065.
11. Marcuse, D., this issue, pp. 1649–1662.
12. Iiguchi, S., Mode Conversion in the Transmission of TE_{01} Wave Through a Slight Tilt and a Slight Offset of Waveguide, J. Inst. Elec. Comm. Engrs. Japan, **40,** 1957, pp. 870–876; 1095–1102.
13. Bresler, A. D., Joshi, G. H. and Marcuvitz, N., Orthogonality Properties for Modes in Passive and Active Uniform Waveguides, J. Appl. Phys. **29,** pp. 794–799.
14. Smythe, W. R., *Static and Dynamic Electricity*, McGraw-Hill Book Co., New York, 1950, p. 98–100.